Innovative (electro-driven) sample preparation tools for metabolomics study of muscle aging

He, Y.

Chapter 6

Metabolomic analysis of dietary-restriction-induced attenuation of sarcopenia in prematurely aging DNA repair-deficient mice

Based on:

Yupeng He, Wei Yang, Luojiao Huang, Marlien van Mever, Rawi Ramautar, Amy Harms, Yvonne Rijksen, Renata M.C. Brandt, Sander Barnhoorn, Kimberly Smit, Dick Jaarsma, Peter Lindenburg, Jan H.J. Hoeijmakers, Wilbert P. Vermeij, Thomas Hankemeier

Metabolomic analysis of dietary-restriction-induced attenuation of sarcopenia in prematurely aging DNA repair-deficient mice.

Journal of Cachexia, Sarcopenia and Muscle (Submitted)

Abstract

Sarcopenia is characterized by loss of skeletal muscle mass and function and is a major risk factor for disability and independence in the elderly. Effective medication is not available. Dietary restriction (DR) has been found to attenuate aging and aging-related diseases, including sarcopenia, but the mechanism of both DR and sarcopenia are yet incompletely understood. In this study, the DR effects on sarcopenia were systematically investigated by applying metabolomics on progeroid DNA repair-deficient *Ercc1*$^{\Delta/-}$ and *Xpg*$^{-/-}$ mice to identify potential biomarkers for attenuation of sarcopenia. The results revealed that metabolites and pathways related to oxidative-stress (9-HODE, 12(S)-HHTrE, and 11-HETE), inflammation (PGE_2, PGD_2, and TXB_2), and muscle growth stimulation ($PGF_{2\alpha}$) are significantly downregulated by DR. On the other hand, several anti-inflammatory metabolites (14,15-DiHETE, 8,9-EET, 12,13-DiHODE and PGF_1), consumption of sources of energy (*i.e.*, muscle and liver glycogen), and energy production pathways (glycolysis, tricarboxylic acid cycle, and gluconeogenesis) are significantly upregulated by DR. The down-modulated muscle growth stimulation metabolite ($PGF_{2\alpha}$) and the increased consumption of glycogen in muscle and liver may be related to the lower mouse body weight by DR. The downregulated oxidative stress, pro-inflammatory mediators, and upregulated anti-inflammatory metabolites resulted in a lower energy expenditure, which contributed to enhanced muscle quality together with upregulated energy production pathways by DR. The improved muscle quality may explain why grip strength is maintained and motor coordination and learning performance are improved by DR in *Ercc1*$^{\Delta/-}$ and *Xpg*$^{-/-}$ mice. This study provides fundamental supporting information on biomarkers and pathways related to the attenuation of sarcopenia, which might facilitate diagnosis, prevention, and clinical therapy of sarcopenia.

1. Introduction

Sarcopenia, the age-related decline of muscle mass and strength, constitutes a major health problem [1, 2], and is one of the main causes of loss of independence in the elderly [2]. Muscle mass usually starts to decline from about 30 years of age, with on average 40% of muscle mass lost by the age of 80 years [3]. Worldwide, 11–50% of those aged 80 or above suffer from sarcopenia [4], and this number is increasing with the linear rise of average life expectancy in the past century. These developments impose severe pressure on healthcare resources and constitute an enormous socio-economic burden [5, 6]. Medication for sarcopenia is unfortunately lacking [7] and the molecular mechanisms underlying sarcopenia are still poorly understood.

Previous studies revealed that oxidative stress and inflammation play important roles in sarcopenia [8, 9], and are associated with the loss of muscle mass [10], and grip strength, an indicator of muscle strength [11]. Energy production related molecules and amino acids were also reported to be associated with muscle contractile function, and other age-associated diseases [12-16]. Several lifestyle interventions can affect health and longevity, including dietary intake and exercise [17]. Among those, caloric- or dietary restriction (CR/DR; reduced food intake without malnutrition) is currently recognized as universal effective intervention for extending lifespan and retarding age-related diseases in numerous species, including mammals [18-22] and humans [23-25]. Colman *et al*. found that DR (with a decrease of caloric intake of 30%) attenuates sarcopenia in rhesus monkeys [22]. Almundarij *et al*. reported that the work efficiency of rat muscle comparably increased after caloric intake was reduced by 50% [26]. Gregorio *et al*. found that CR significantly attenuated age-related loss of motor neurons and turnover of muscle fibers in old mice [27]. Young *et al*. reported that 40% of DR attenuates age-related muscle atrophy in accelerated aging (*Sod1*$^{-/-}$) mice [28]. However, the fundamental mechanism of how DR attenuates sarcopenia still needs to be systematically investigated to identify potential biomarkers for monitoring diagnosis, prevention, and treatment of sarcopenia.

Aging and age-related diseases can be influenced by many factors [29]. One of the main causal hallmarks of aging is time-dependent accumulation of DNA damage, also known as genomic instability [29-32]. Mice deficient in the DNA excision-repair genes *Ercc1* (*Ercc1*$^{\Delta/-}$) or *Xpg* (*Xpg*$^{-/-}$) cannot properly repair multiple types of DNA lesions leading to an accelerated accumulation of persisting DNA damage, which stall elongating RNA

polymerases causing transcription stress, leading to reduced and gene-length dependent transcriptional decline particularly in post-mitotic tissues [21, 33]. Importantly, genome-wide transcription stress causing lowered and skewed transcriptional output has subsequently also been discovered in normal aging in mice and to be widely evolutionary conserved from worms to man [33], demonstrating the value of progeroid DNA repair deficient mouse mutants for understanding the natural process of aging [30]. Since transcription is at the basis of all cellular processes, and transcription stress triggers a complex DNA damage response [34], it has numerous secondary and tertiary consequences. This explains the wide range of pathological, physiological, and behavioral features associated with the multi-morbidity of natural aging and the dramatic accelerated aging in repair mouse mutants and corresponding human syndromes, including progressive neurodegeneration (dementia, ataxia, hearing and vision loss); osteoporosis; liver, kidney, vascular and hematological ageing; etc. [21, 33, 35-38]. Progeroid *Ercc1*$^{\Delta/-}$ mice were previously successfully used for studying and modulating many features of aging [21] including sarcopenia [39].

Metabolite profiling is an important tool to link genotype and phenotype, and hence constitutes a powerful approach for the investigation of complex diseases and identification of diseases' biomarkers [40], such as oxidative stress and inflammatory markers (*e.g.*, some signaling lipids), and energy status (ATP, ADP, glucose, etc.). Therefore, in this paper, metabolomics was utilized to systematically investigate metabolites related to oxidative stress, (pro- and anti-) inflammatory status, and energy production and consumption in wild type, *Ercc1*$^{\Delta/-}$ and *Xpg*$^{-/-}$ mouse models under *ad libitum* fed and DR conditions. Overall, this work provides insight into metabolic mechanisms of the DR effects on sarcopenia, supplies reference information for the potential biomarkers of sarcopenia attenuation, and facilitate the diagnosis, prevention, and treatment of sarcopenia.

2. Methods

2.1 Mouse models

The generation and characterization of *Ercc1*$^{\Delta/+}$ and *Ercc1*$^{+/-}$ mice have been previously described [41]. *Ercc1*$^{\Delta/-}$ mice were obtained by crossing *Ercc1*$^{\Delta/+}$ (in a pure C57BL6J or FVB background) with *Ercc1*$^{+/-}$ mice (in a pure FVB or C57BL6J background respectively) to yield *Ercc1*$^{\Delta/-}$ offspring with a genetically uniform F1 C57BL6J/FVB hybrid background. *Xpg*$^{-/-}$ mice have been generated and characterized previously [38] and were similarly

obtained by crossing *Xpg*$^{+/-}$ (in a pure C57BL6J background) with *Xpg*$^{+/-}$ mice (in a pure FVB background). Wild-type F1 littermates (from *Ercc1*$^{\Delta/-}$ and *Xpg*$^{-/-}$ breedings) were used as controls. Hence, all animals used in the studies described here were of the same F1 C57BL6J/FVB hybrid genetic background. Typical unfavorable characteristics, such as blindness in an FVB background or deafness in a C57BL6J background, do not occur in this hybrid background. Only male mice were used in this paper to minimize the influence of gender on DR study.

All of the animals used were in accordance with the Principles of Laboratory Animal Care and with the guidelines approved by the Dutch Ethical Committee (permit no. 139-12-13, 139-12-18, 17-867-10, and 18-6886-05), in full accordance with European legislation.

2.2 Dietary intervention and housing conditions

Mice were housed in individual ventilated cages under specific pathogen-free conditions (20–22°C, 12–12 h light–dark cycle with light phase adjusted to between 24:00 and 12:00 h) and provided food and water *ad libitum* (AL). Because the *Ercc1*$^{\Delta/-}$ and *Xpg*$^{-/-}$ mice were smaller, food was administered within the cages, and water bottles with long nozzles were used from around 2 weeks of age. Mice were weighed, visually inspected weekly, and scored blindly for gross morphological and motor abnormalities weekly. All efforts were made to ameliorate the suffering of the animals. Animals were bred and maintained on AIN93G synthetic pellets (Research Diet Services B. V.; gross energy content 4.9 kcal/g dry mass, digestible energy 3.97 kcal/g). Animals were divided randomly over all groups to prevent selection bias. Dietary restriction (DR) was applied as published before [21]. On average, *Ercc1*$^{\Delta/-}$ and *Xpg*$^{-/-}$ mice ate 2.3 g food per day. DR was initiated gradually starting from 7 weeks of age with 10% food reduction (2.1 g/day), when animals reached almost-maximum bodyweight and development was completed, and was increased weekly by 10%, until it reached 30% DR (1.6 g/day) from 9 weeks of age until 16 weeks. Wild-type (WT) mice ate on average 3.0 g food per day, resulting in 2.1 g/day for 30% DR. Food was given to the animals just before the start of the dark (active) period, Zeitgeber Time (ZT) 12:00, to minimize disturbance of the biological clock. All mice were sacrificed and muscle samples were collected within a time frame of 1-3.5 hours after feeding in their active period, between ZT 13:00 and 15:30, to avoid nutritional or circadian fluctuations of metabolites due to differences in the time after feeding and the biological clock.

2.3 Behavioral analyses

Motor coordination performance was assessed by measuring the average time spent on an (2-40 rpm) accelerating rotarod (Ugo Basile). All animals were given four consecutive trials of a maximum of 5 min with inter-trial intervals of 1 h. Grip strength was determined by placing mice with forelimbs or all limbs on a grid attached to a force gauge, and steadily pulling the mice by their tail. Grip strength is defined as the maximum strength produced by the mouse before releasing the grid. For each value the test was performed in triplicate. Behavioral assays (motor coordination and grip strength) were measured in the week at 16 weeks and 14 weeks of age for *Ercc1*$^{\Delta/-}$ and *Xpg*$^{-/-}$, respectively. 50% of WT mice were assessed and collected at the same time as the *Xpg*$^{-/-}$ mice and 50% with the *Ercc1*$^{\Delta/-}$ mice, but this two weeks difference did not yield into any trend difference in motor coordination performance nor grip strength. Body weight was also determined just before mice collection.

2.4 Muscle tissue isolation and blood glucose measurement

Mice were anaesthetized using CO_2 and a large piece of quadriceps femoris muscle (Quad) was dissected and rapidly frozen in liquid nitrogen, then stored in -80°C before analysis. Blood glucose was determined with a Freestyle mini blood glucose meter just before mice collection [21].

2.5 Metabolomic analysis preparation

2.5.1 Chemicals and internal standards (ISTDs)

The chemicals, solvents, and ISTDs used for muscle tissue extraction were described in Chapter 5. Butylated hydroxytoluene (BHT) and methyl tert-butyl ether (MTBE) were obtained from Sigma-Aldrich (Steinheim, Germany). 1-butanol was purchased from Acros Organics (Geel, Belgium). MilliQ water was obtained from a Millipore high-purity water dispenser (Billerica, MA, USA). All solvents were HPLC grade or higher. For internal standards (ISTDs), stable isotope (deuterium-, carbon-, and/or nitrogen-) labelled metabolites were used. Labelled oxylipins, fatty acids, and endocannabinoids ISTDs were acquired from Cayman Chemicals (Ann Arbor, MI, USA) (Table S1 in the Supplementary Information). Labelled ATP, AMP and UTP were purchased from Sigma-Aldrich (Steinheim, Germany). Labelled amino acid and organic acids ISTDs were ordered from Cambridge Isotope Laboratories (Andover, MA, USA) (Table S2).

For the lipid ISTDs, the stock solution was prepared in MeOH in a stated concentration (Table S1) containing 0.4 mg/mL BHT . For the stock solution of metabolites related to energy production, the ISTDs were prepared in MilliQ water in stated concentration in Table S2.

2.5.2 Muscle tissue extraction

The muscle tissue extraction method was performed for all muscle samples as described in Chapter 5. Briefly, muscle tissues were lyophilized in a CHRIST (Alpha 3-4 LSC basic) freeze-dryer (Osterode am Harz, Germany; connected to a Vacuubrand Chemistry Hybrid Pump RC6 high vacuum pump, Wertheim, Germany) for 24 hours, and weighed. 100 mg (± 10%) zirconium oxide beads (0.5 mm; Next Advance, Averill Park, NY, USA) was utilized for dry-homogenization of muscle tissues in a Bullet Blender (BBX24; Next Advance, Averill Park, NY, USA) for 15 min at speed 9. 10 µL labelled ISTDs of lipids (Table S1) and energy production related metabolites (Table S2) were spiked in the muscle tissues before extraction to correct the potential bias during sample extraction.

5 µL antioxidant solution (0.4mg/mL BHT:EDTA=1:1), 400 µL of cold MilliQ water, and 1 mL organic solvent (BuOH: MTBE=1:1, v/v) were added to all samples, and settled on ice for 20 min before the homogenization by Bullet Blender for 15 min at speed 9. Then the homogenized samples were centrifuged (2,000×g, 4 ℃) for 10 min. 900 µL and 200 µL of the upper organic and lower aqueous phase were collected, respectively, evaporated and reconstituted to 50 µL MeOH for organic phase and 100 µL 50% MeOH (50% MilliQ Water) for aqueous phase.

2.6 Metabolite analysis

A portion of extracted mouse muscle tissue for pre-experiment was used as quality control (QC) samples. A QC sample was injected once each 6-8 samples to evaluate and correct for changes in sensitivity of the instruments.

2.6.1 Lipid metabolite analysis

The lipid metabolites were analyzed by a validated ultra-performance liquid chromatography tandem mass spectrometry (UPLC-MS/MS) method [43]. Briefly, each sample was measured with two complementary reverse phase methods using mobile phases with different pH.

The low pH run utilized an Acquity BEH C18 column (50 × 2.1 mm, 1.7 µm; Waters, USA) on a Shimadzu LC-30AD (Japan) hyphenated to a SCIEX Q-Trap 6500+ (Framingham, MA, USA) Separations were performed using three mobile phases: (A) water with 0.1% acetic acid; (B) ACN: MeOH (9:1, v/v) with 0.1% acetic acid; (C) Isopropanol with 0.1% acetic acid at 40 °C at a flow rate of 0.7 mL/min. The 16 minute run used the following gradient: start with 20% B and 1% C; B was increased to 85% between 0.75 and 14 min, and C was increased to 15% between 11 and 14 min; the condition held for 0.5min prior to column re-equilibration at the starting conditions from 14.8 to 16 min. Data was acquired using Sciex Analyst software (Version 1.7, Framingham, MA, USA) and peak integration used Sciex OS (Version 1.4.0, Framingham, MA, USA).

The high pH run used a Kinetex® Core-Shell EVO 100 Å C18 column (50 × 2.1 mm, 1.8 µm; Phemomenex, USA) on a Shimadzu LCMS-8060 system (Shimadzu, Japan). Separations used mobile phases (A) 5% ACN with 2 mM ammonium acetate and 0.1% ammonium hydroxide and (B) 95% ACN with 2 mM ammonium acetate and 0.1% ammonium hydroxide at 40 °C at a flow rate of 0.6 mL/min. The gradient started with 1% B; B was increased to 100% from 0.7 to 7.7 min; 100% B hold for 0.75 min prior to re-equilibration at the starting conditions between 8.75 and 11 min. Data was acquired and peaks integrated using LabSolutions (Version 5.97 SP1, Shimadzu, Japan). Multiple reaction monitoring (MRM) was utilized in MS/MS acquisition in both positive and negative electrospray ionization mode with polarity switching for low and high pH method.

2.6.2 Energy production related metabolites analysis

The energy production related metabolites were analyzed by a hydrophilic interaction liquid chromatography (HILIC) mass spectrometry platform [44]. Briefly, a Waters UPLC (AcquityTM, Milford, MA, USA) coupled with a SeQuant ZIC- cHILIC column (PEEK 100 × 2.1 mm, 3.0 µm particle size; Merck KGaA, Darmstadt, Germany) at 30 °C and a Sciex MS (Triple-TOF 5600+, Framingham, MA, USA) was applied for a separation method: (A) 90% acetonitrile with 5 mM ammonium acetate at pH 6.8; (B) 10% acetonitrile with 5 mM ammonium acetate at pH 6.8, at a flow rate of 0.25 mL/min with the gradient method: 100% A for 2 min; ramping 3–20 min to 60% A; ramping 20–20.1 to 100% A and re-equilibrated to 35 min with 100% A. The MS data was acquired at full scan range 50–900 m/z in negative ionization mode with curtain gas 270.96 kPa, source temperature

400 °C and ion source voltage 4.64 kV by Sciex Analyst (Version 1.7, Framingham, MA, USA) and peak integration used Sciex OS (Version 1.4.0, Framingham, MA, USA). β-hydroxybutyrate, reduced glutathione (GSH) and oxidized glutathione (GSSG) were also analyzed by HILIC-MS method.

2.7 Data analysis

For each metabolite analyzed by UPLC-MS(/MS), the response ratio was obtained by Equation 1, normalized by the muscle tissue dry weight, and corrected by the QC samples:

$$Response\ ratio = \frac{Peak\ area\ of\ the\ target\ metabolite}{Peak\ area\ of\ the\ assigned\ ISTD} \div muscle\ tissue\ dry\ weight \quad \text{(Equation 1)}$$

For metabolites that can be measured by multiple platforms, *i.e.*, some fatty acids can be determined with both low and high pH lipid method, the results with smaller QC RSD were utilized (Table S1).

The fold change of metabolites regulated by DR was calculated by the Equation 2:

$$Fold\ change = \frac{Response\ ratio\ of\ DR}{Response\ ratio\ of\ AL} \quad \text{(Equation 2)}$$

RStudio (Version 1.4.1106) and R (Version 4.0.5) was used for data statistical analysis, and figure plotting.

3. Results

We examined first the effects of accelerated aging and DR on mouse body weight and muscle functioning, *i.e.*, grip strength, motor learning and coordination in WT and progeroid DNA-repair-deficient mice. Subsequently, the mechanism of DR was investigated by analyzing major classes of molecules relevant for muscle function and quality, *i.e.*, oxidative stress, pro- and anti-inflammatory markers, and energy status. Since mouse behavior and metabolic parameters are strongly influenced by the time of the circadian clock and by the nutritional status, particularly in the DR group, which receives only once a day all food, we used a standardized protocol for feeding the DR mice just before the start of their nocturnal (*i.e.*, active, ZT 12:00) period to not disturb their biological rhythm. Moreover, since we are most interested in the long-term effect of dietary restriction independent of the actual nutritional status, we opted for collecting the mice ~1-3.5 hours after feeding (ZT ~13:00-15:30), when they had just finished or were finishing their food. In his manner the moment in the circadian day was comparable for all mice and a state of

fasting was avoided which otherwise would have depended on the time since the last food intake.

3.1 Differential effects of DR on mouse body weight and muscle functioning

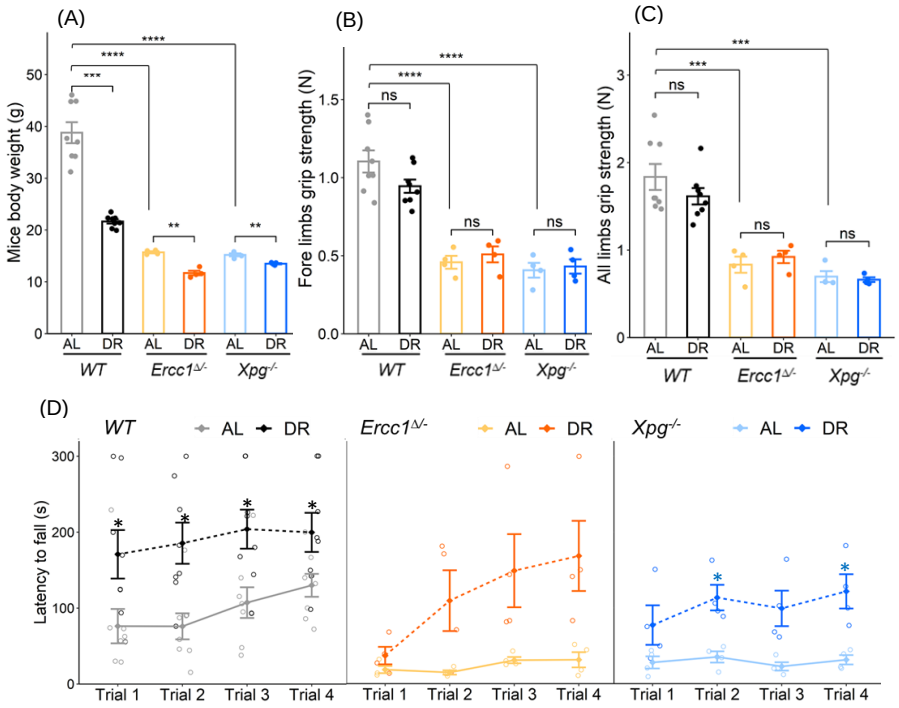

Figure 1. The effects of dietary restriction on body weight, grip strength, and motor coordination in *WT* (n=8), *Ercc1*$^{\Delta/-}$ (n=4), and *Xpg*$^{-/-}$ (n=4) mice with only male and age 14/16 weeks. *p < 0.05, **p < 0.01, ***p < 0.001, t test with false discovery rate (FDR) correction.

(A) Mouse body weight, (B) Fore limbs grip strength, (C) All limbs grip strength, (D) Motor learning and coordination performance. (Trial 1, 2, 3 and 4 means the 1st, 2nd, 3rd, and 4th trial, respectively)

To investigate the effects of dietary restriction (DR, starting at the age of 7 weeks) on sarcopenia, we initially monitored mouse body weight, grip strength, and accelerating rotarod performance in 16-week-old *Ercc1*$^{\Delta/-}$ mice and 14-week-old *Xpg*$^{-/-}$ mice, with corresponding WT littermates. These ages correspond to approximately 75% of their maximum lifespan and at which both mouse models display progressive age-related pathologies across many organs, including severe muscle wasting [35, 38, 39, 45]. Under *Ad Libitum* (AL) feeding conditions, body weight of *Ercc1*$^{\Delta/-}$ and *Xpg*$^{-/-}$ mice was substantially lower compared to WT littermates, and all were significantly decreased ($p<0.01$) by DR, ranging from 11% to 44% (Figure 1A), consistent with previous data [21]. *Ercc1*$^{\Delta/-}$ and *Xpg*$^{-/-}$ mice already show a reduced muscle strength (Figure 1B and 1C), which might be the result of their lower body weight (Figure 1A) and muscle wasting phenotype [39]. However, DR did not affect their fore limbs and all limbs grip strength in the progeroid mutants, while showing a trend of reduced strength in WT animals (Figure 1B and 1C). One of the detrimental effects of sarcopenia in the elderly is loss of motor coordination [46]. To further investigate how motor coordination and learning performance in progeroid mice can be modulated by DR, four trials of accelerating rotarod performance were conducted. In line with their accelerated aged phenotype, AL-fed *Ercc1*$^{\Delta/-}$ and *Xpg*$^{-/-}$ mice showed a reduced motor coordination compared to WT mice (Figure 1D), consistent with the adverse effect of sarcopenia on motor coordination, and fully in line with previous observations [39, 46]. DR strongly ($p<0.05$) improved the motor coordination and learning in all mouse models (Figure 1D). Especially *Ercc1*$^{\Delta/-}$ and *Xpg*$^{-/-}$ mice were able to equally control motor coordination as normal WT mice simply by lowering food intake. *Ercc1*$^{\Delta/-}$ DR mice were poor in rotarod performance at the first trial but systematically improved. Since these mice have a longer lifespan than the *Xpg*$^{-/-}$ mice and they seem to profit more from DR than the *Xpg*$^{-/-}$ mutants [21], which are already more advanced in overall aging compared to *Ercc1*$^{\Delta/-}$ at the moment of the start of DR. In fact, this indicates that the neurological performance in *Ercc1*$^{\Delta/-}$ mice is strongly improving.

3.2 The effects of accelerated aging on oxidative stress related, pro-inflammatory, anti-inflammatory, and energy related metabolites.

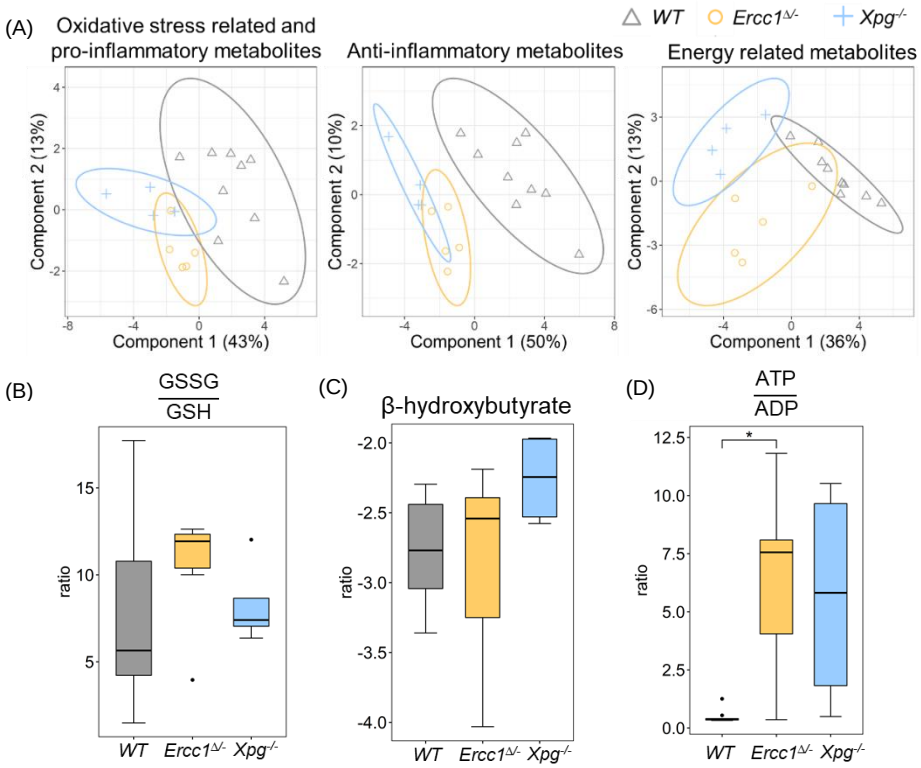

Figure 2. (A) The partial least squares-discriminant analysis (PLS-DA) score plot for the effect of accelerated aging on oxidative stress related, pro-inflammatory, anti-inflammatory, and energy related metabolites in AL mice; the effects of accelerated aging on the representative indicators of (B) oxidative stress and pro-inflammation, (C) anti-inflammation, and (D) energy status. *WT* (n=9), *Ercc1*$^{\Delta/-}$ (n=5), and *Xpg*$^{-/-}$ (n=4). *p < 0.05, t test with FDR correction.

The significantly decreased fore and all limbs grip strength, motor coordination and learning performance in the AL progeroid mice muscle comparing with AL-WT mice (Figure 1) may be related to altered muscle function and quality. Hence, molecules related to muscle function and quality, *i.e.*, oxidative stress, pro- and anti-inflammatory markers, and energy status, were analyzed by Partial Least Squares Discriminant Analysis (PLS-DA) following a method recently developed for the simultaneous detection of signaling lipids and polar metabolites in small quantities, e.g. muscle biopsies of the quadriceps femoris muscle (Quad), to profile the effects of accelerated aging on these metabolites [42]. We choose the Quad for systematic analysis because of its overall stability of metabolites and larger muscle size [42]. Separation between WT and *Ercc1*$^{\Delta/-}$ or *Xpg*$^{-/-}$ mice was observed, especially for the anti-inflammatory metabolites (Figure 2A), indicating large alterations of accelerated aging in these metabolites.

Three indicators of oxidative stress, anti-inflammation, and energy status were used to profile the effects of accelerated aging. The ratio of oxidized glutathione (GSSG) to reduced glutathione (GSH) is used as an important marker of oxidative stress [47]. Nonsignificant increase of GSSG/GSH in *Ercc1*$^{\Delta/-}$ (or *Xpg*$^{-/-}$) mice compared to WT mice (Figure 2B) may be related to the mice improved oxidation defense, *i.e.*, the large increase of β-hydroxybutyrate (Figure 2C), an important indicator to exhibit the anti-aging effects [48, 49]. The significantly ($p<0.05$) elevated ratio of ATP to ADP in *Ercc1*$^{\Delta/-}$ and *Xpg*$^{-/-}$ mice may be related to the increased transcription stress in the progeroid mice (Figure 2D), which reduced the consumption of ATP and resulted in a higher energy status. Similar results were also observed in the *Ercc1*$^{\Delta/-}$ and *Xpg*$^{-/-}$ mice liver by Milanese *et al.* [50]. Further metabolomics investigations were conducted to explore the DR effects on these oxidative stress, anti-inflammation, and energy-status-related molecules.

3.3 The effects of DR on pro-inflammatory, oxidative stress related, and muscle growth stimulation metabolites and pathways.

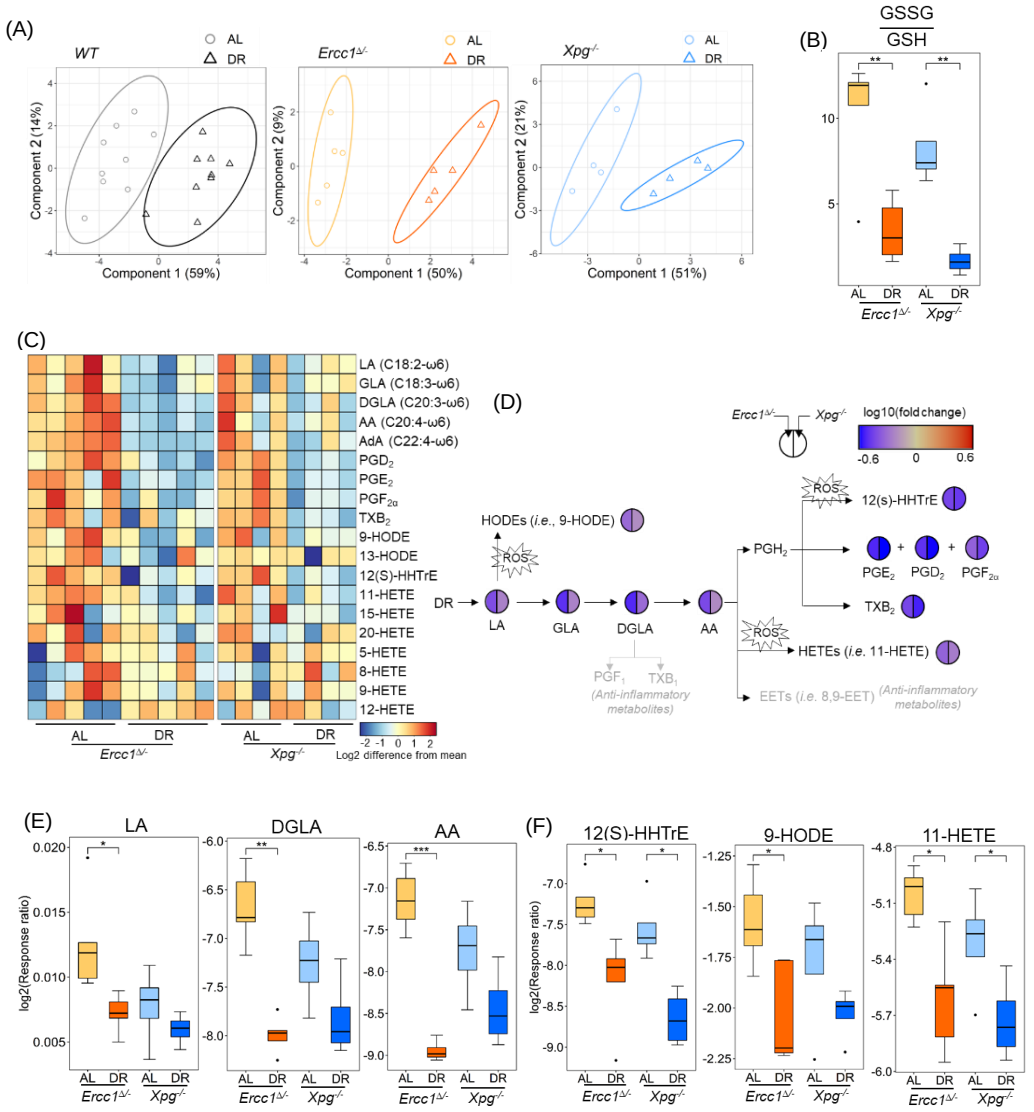

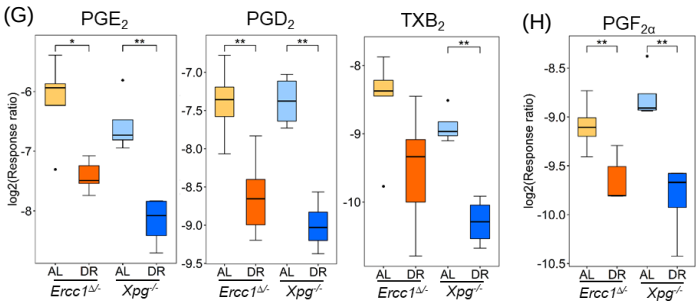

Figure 3. Footprint of the effects of DR on pro-inflammatory and oxidative stress related pathways and metabolites for sarcopenia in *WT* (n=9), *Ercc1*$^{\Delta/-}$ (n=5), and *Xpg*$^{-/-}$ (n=4) mice.

(A) The PLS-DA score plot for the effect of DR on pro-inflammatory and oxidative stress related metabolites;

(B) The effects of DR on oxidative stress indicator, the ratio of GSSG to GSH in *Ercc1*$^{\Delta/-}$ and *Xpg*$^{-/-}$ mouse muscle. **p < 0.01, ***p < 0.001, t test with FDR correction;

(C) Heatmap representation of the pro-inflammatory and oxidative stress related metabolites between AL and DR in *Ercc1*$^{\Delta/-}$ and *Xpg*$^{-/-}$ mouse muscle;

(D) The fold change of metabolites significantly (p<0.05) regulated by DR in the pro-inflammatory pathways (t test with FDR correction);

The effects of DR on (E) ω6 polyunsaturated fatty acids, (F) ROS stimulated metabolites, (G) pro-inflammatory metabolites, and (H) muscle growth stimulation metabolite ($PGF_{2\alpha}$) in *Ercc1*$^{\Delta/-}$ and *Xpg*$^{-/-}$ mouse muscle. *p < 0.05, **p < 0.01, ***p < 0.001, t test with FDR correction.

To identify the fundamental molecular changes of DR on inflammation and oxidative stress in sarcopenia, lipidomics analysis was performed on muscle biopsies of sarcopenic *Ercc1*$^{\Delta/-}$ and *Xpg*$^{-/-}$ animals and WT controls. We measured pro-inflammatory and oxidative-stress-related metabolites, and lipid peroxidation products for which *Ercc1*$^{-/-}$ mouse embryonic fibroblasts and mice have been reported to be hypersensitive [51], *i.e.*, ω6 polyunsaturated fatty acids (PUFAs) [52]. In addition, we examined prostaglandin (PG) series-2 [52, 53], thromboxanes (TX) series-2 [52, 54], hydroxyoctadecadienoic acids (HODEs) [55, 56], 12(S)-hydroxyheptadecatrienoic acid (HHTrE) [57], and hydroxyeicosatetraenoic acids (HETEs) [58, 59]. The resulting metabolic profiles of PLS-DA showed overall clear differences between AL and DR in *Ercc1*$^{\Delta/-}$ and *Xpg*$^{-/-}$ mice (Figure 3A), indicating that DR exerts large effects on pro-inflammatory and oxidative-stress-related metabolites in the

progeroid mice muscle. This is consistent with the very strong anti-aging effect of DR in the progeroid repair mutants [21]. In view of the high impact of DR in the *Ercc1*$^{\Delta/-}$ and *Xpg*$^{-/-}$ mice, we decided to investigate the effect of DR in more detail. Significantly ($p<0.01$) decreased GSSG/GSH in *Ercc1*$^{\Delta/-}$ and *Xpg*$^{-/-}$ mice demonstrated reduced oxidative stress by DR in progeroid mice (Figure 3B). The heatmap profiles were used to further analyze the metabolites (Table S3 in the Supplementary Information) related to oxidative stress and pro-inflammation. The results clearly show an overall reduction by DR in both *Ercc1*$^{\Delta/-}$ and *Xpg*$^{-/-}$ mice (Figure 3C). To better visualize the DR effects, the fold change (Equation 2) of significantly ($p<0.05$) regulated metabolites were profiled in the schematic pathways related to pro-inflammatory and oxidative stress (Figure 3D). The results revealed that the linoleic acid (LA) and arachidonic acid (AA) pathways related to pro-inflammatory and oxidative stress were all significantly and consistently downregulated by DR in both models.

LA, one of the two essential fatty acids for animals and human [60, 61], must be obtained from food. DR significantly ($p<0.05$) decreased LA in progeroid mouse muscle tissues, fully in line with their reduced food intake, concomitant with a notable ($p<0.001$) decline of its downstream ω6 PUFAs, *i.e.*, dihomo-γ-linolenic acid (DGLA) and AA (Figure 3E). Since mice were sacrificed and samples collected 1-3.5 hours after feeding, the influence of fasting on the decreased LA and its downstream ω6 PUFAs was minimized. HODEs, *i.e.*, 9-HODE, are stable indicators of oxidative stress and strong regulators of inflammation [55, 56]. Peroxide plays an important role in the generation of 12(S)-HHTrE [57], and 11-HETE is reportedly formed through auto-oxidative reactions [59]. Significantly decreased 9-HODE, 12(S)-HHTrE, and 11-HETE demonstrated lower levels of oxidative stress by DR in *Ercc1*$^{\Delta/-}$ and *Xpg*$^{-/-}$ mice (Figure 3F). PG series-2, *i.e.*, PGE_2, PGD_2, and $PGF_{2\alpha}$ [52, 53], and TX series-2, *i.e.*, TXB_2 [52, 54], are reported as metabolites promoting inflammation. Markedly decreased PGE_2, PGD_2, TXB_2 (Figure 3G), and $PGF_{2\alpha}$ (Figure 3H) demonstrated that DR alleviated the pro-inflammatory status in *Ercc1*$^{\Delta/-}$ and *Xpg*$^{-/-}$ mice. Additionally, $PGF_{2\alpha}$ is also reported as a stimulator of skeletal muscle cell growth [62, 63]. Downregulated $PGF_{2\alpha}$ by DR may simultaneously contribute to the decreased body weight of the repair mutants (Figure 1A) and supports the theory of temporarily suppressing growth to redirect energy sources more towards resilience, maintenance and (anti-oxidant) defense mechanisms [21, 64, 65].

3.4 The effects of DR on anti-inflammatory metabolites and pathways.

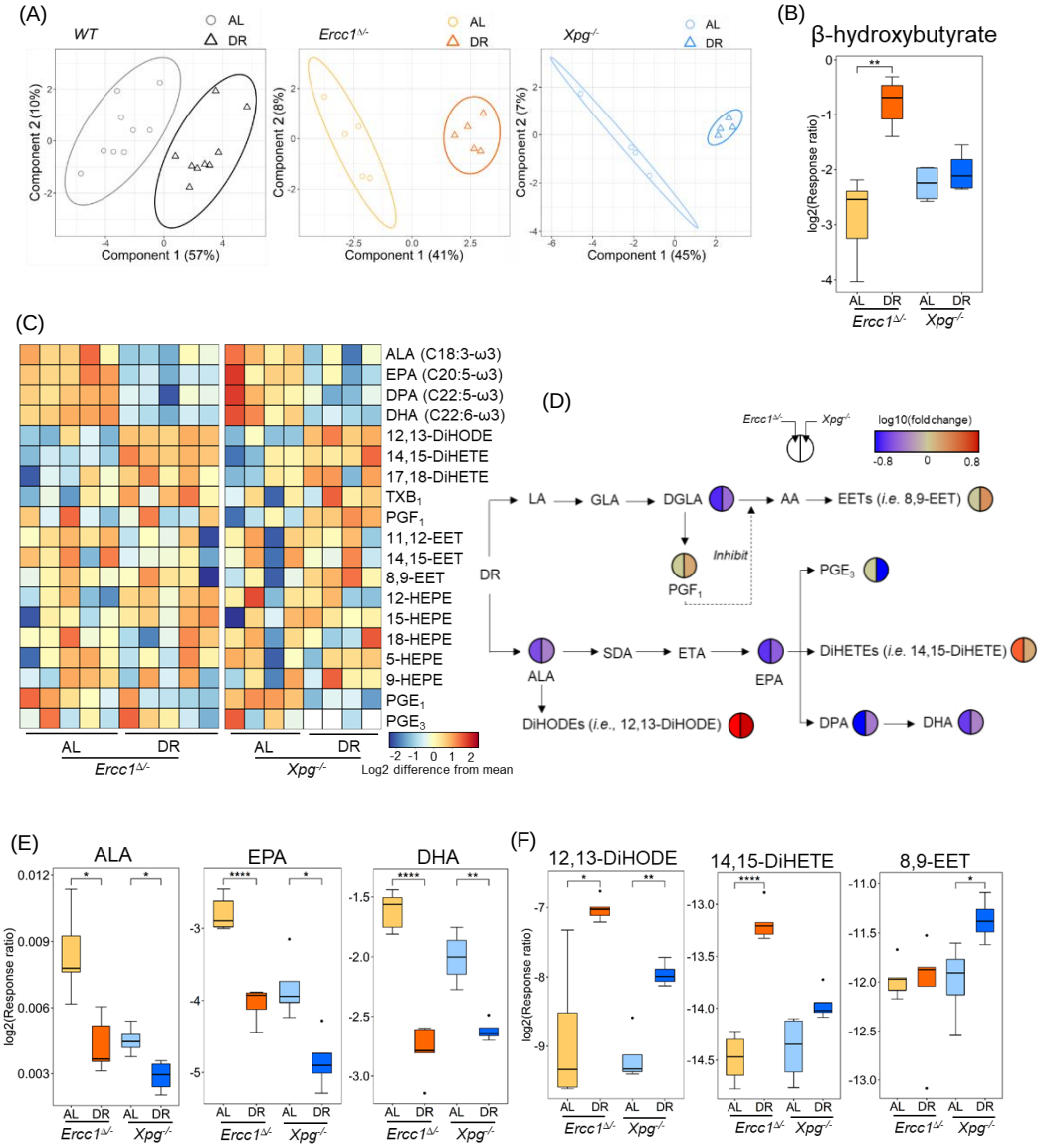

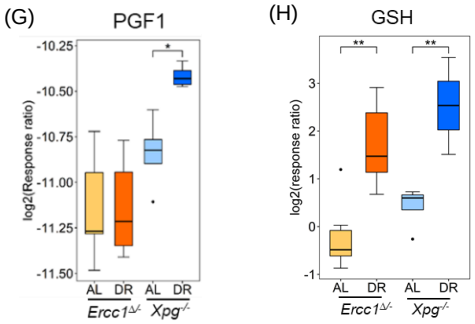

Figure 4. Footprint of the effects of DR on anti-inflammatory metabolites and pathways for sarcopenia in *WT* (n=9), *Ercc1*$^{\Delta/-}$ (n=5), and *Xpg*$^{-/-}$ (n=4) mice.

(A) The PLS-DA score plot for the effect of DR on anti-inflammatory metabolites;

(B) The effects of DR on anti-aging exhibition molecule (β-hydroxybutyrate) in *Ercc1*$^{\Delta/-}$ and *Xpg*$^{-/-}$ mouse muscle. ***p < 0.001, t test with FDR correction;

(C) Heatmap profile of the anti-inflammatory metabolites between AL and DR in *Ercc1*$^{\Delta/-}$ and *Xpg*$^{-/-}$ mouse muscle (background color was used for the non-detected metabolites);

(D) The fold change of metabolites significantly (p<0.05) regulated by DR in the anti-inflammatory pathways (t test with FDR correction);

The effects of DR on (E) ω3 polyunsaturated fatty acids, (F) anti-inflammatory metabolites, (G) metabolites in LA pathway to inhibit the AA generation, and (H) GSH in *Ercc1*$^{\Delta/-}$ and *Xpg*$^{-/-}$ mouse muscle. *p < 0.05, **p < 0.01, ***p < 0.001, ****p < 0.0001, t test with FDR correction.

The altered concentrations of oxidative stress markers and pro-inflammation signaling lipids associated with DR may be not only due to the reduced levels of reactive oxygen species (ROS) or reactive nitrogen species (RNS), but also caused by the modulation of anti-inflammatory cytokines [66], which presented protective antioxidant defenses in *Ercc1*$^{\Delta/-}$ and *Xpg*$^{-/-}$ mice [50], such as eicosapentaenoic acid (EPA) [52, 67], PG series-1 and series-3 [52, 68], TX series-1 [52, 68], epoxyeicosatrienoic acids (EETs) [69], hydroxyeicosapentaenoic acids (HEPEs) [70, 71], dihydroxy-eicosatetraenoic acids (DiHETEs) [72], and potential anti-inflammatory mediators, dihydroxy octadecadienoic acids (DiHODEs) [73, 74]. PLS-DA profiles of these anti-inflammatory metabolites clearly segregated AL and DR groups in *Ercc1*$^{\Delta/-}$ and *Xpg*$^{-/-}$ mice (Figure 4A), demonstrating the more potent robustness in regulation of anti-inflammatory mediators by DR in the muscle of progeroid mice. β-hydroxybutyrate is reported as an important marker of the anti-aging

effects of DR and fasting [48, 49]. Significantly ($p<0.001$) increased β-hydroxybutyrate indicated improved anti-inflammation by DR in progeroid *Ercc1*$^{\Delta/-}$ mice (Figure 4B). The heatmap profile of analyzed anti-inflammation metabolites (Table S4) in *Ercc1*$^{\Delta/-}$ and *Xpg*$^{-/-}$ muscle showed an obvious downregulation of ω3 PUFAs (*i.e.*, α-Linolenic acid (ALA), EPA, docosapentaenoic acid (DPA), and docosahexaenoic acid (DHA)), and several clearly upregulated anti-inflammatory mediators (*i.e.*, 14,15-DiHETE, 17,18-DiHETE, TXB_1, PGF_1, and 12,13-DiHODE) by DR in the progeroid sarcopenic mice (Figure 4C). Using a cut-off p-value of <0.05 for the fold change (Equation 2) of metabolites, we clearly observed significantly down-regulated (*i.e.*, ALA, EPA, DPA, DHA, and PGE_3), and up-regulated mediators (*i.e.*, PGF_1, 8,9-EET, 12,13-DiHODE, and 14,15-DiHETE) by DR in the anti-inflammation-related pathways in *Ercc1*$^{\Delta/-}$ and *Xpg*$^{-/-}$ mice (Figure 4D).

As ALA is the other essential fatty acid for animals and human [60, 61] which needs to be obtained from the food, our data show a clear, significant ($p<0.05$) decrease of ALA by DR. Subsequently, this may result is a significant decline of its downstream anti-inflammatory ω3 PUFAs, *i.e.*, EPA and DHA, and also PGE_3 (Figure 4E). Our experimental protocol minimized the influence of fasting on the decreased ALA and these ω3 PUFAs by sacrificing mice and isolating muscle samples 1-3.5 hours after feeding, and also diminished fluctuations of ω3 PUFAs due to perturbing the biological clock. However, some metabolites inhibiting inflammation, *i.e.*, 14,15-DiHETE [72] and 12,13-DiHODE [73, 74], were notably upregulated by DR despite that the metabolites they are generated from, *i.e.*, EPA and ALA, were downregulated (Figure 4F). PGF_1, the product of DGLA, is able to inhibit AA synthesis from DGLA [52]. The other anti-inflammatory mediator, 8,9-EET, is generated from AA [69]. PGF_1 (Figure 4G) and 8,9-EET (Figure 4F) were all significantly ($p<0.05$) increased by DR even though the metabolites they are derived from (*i.e.*, DGLA and AA) were notably down-modulated in *Ercc1*$^{\Delta/-}$ and *Xpg*$^{-/-}$ mice (Figure 3D and 3E). Reduced glutathione (GSH) is considered as an old antioxidant [75]. Significantly ($p<0.01$) increased GSH also indicated the improved anti-inflammation by DR in *Ercc1*$^{\Delta/-}$ and *Xpg*$^{-/-}$ mice (Figure 4H). Notably, increased β-hydroxybutyrate and GSH by DR in muscle, and the upregulated anti-inflammatory mediators in *Ercc1*$^{\Delta/-}$ and *Xpg*$^{-/-}$ mice demonstrated that DR improved the anti-inflammatory defense in the progeroid mice.

3.5 The effects of DR on energy production related metabolites and pathways.

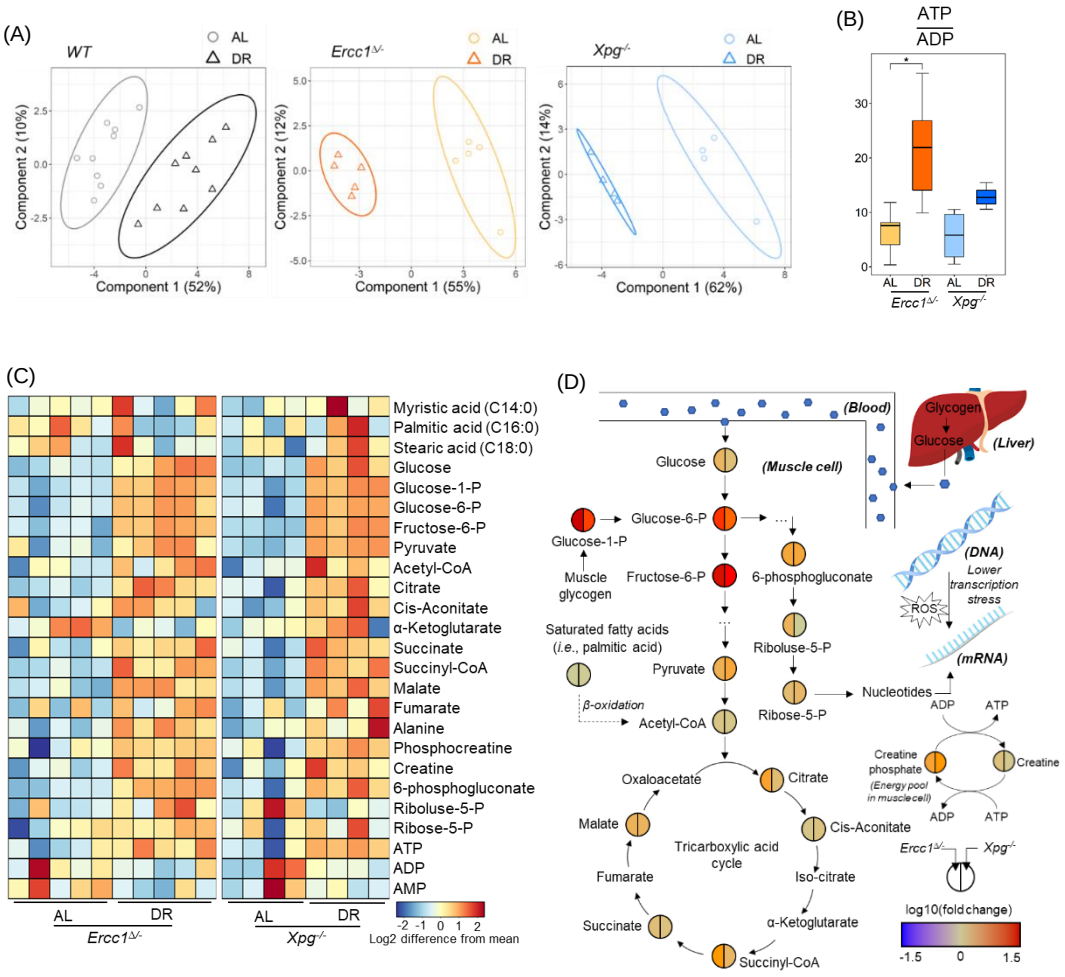

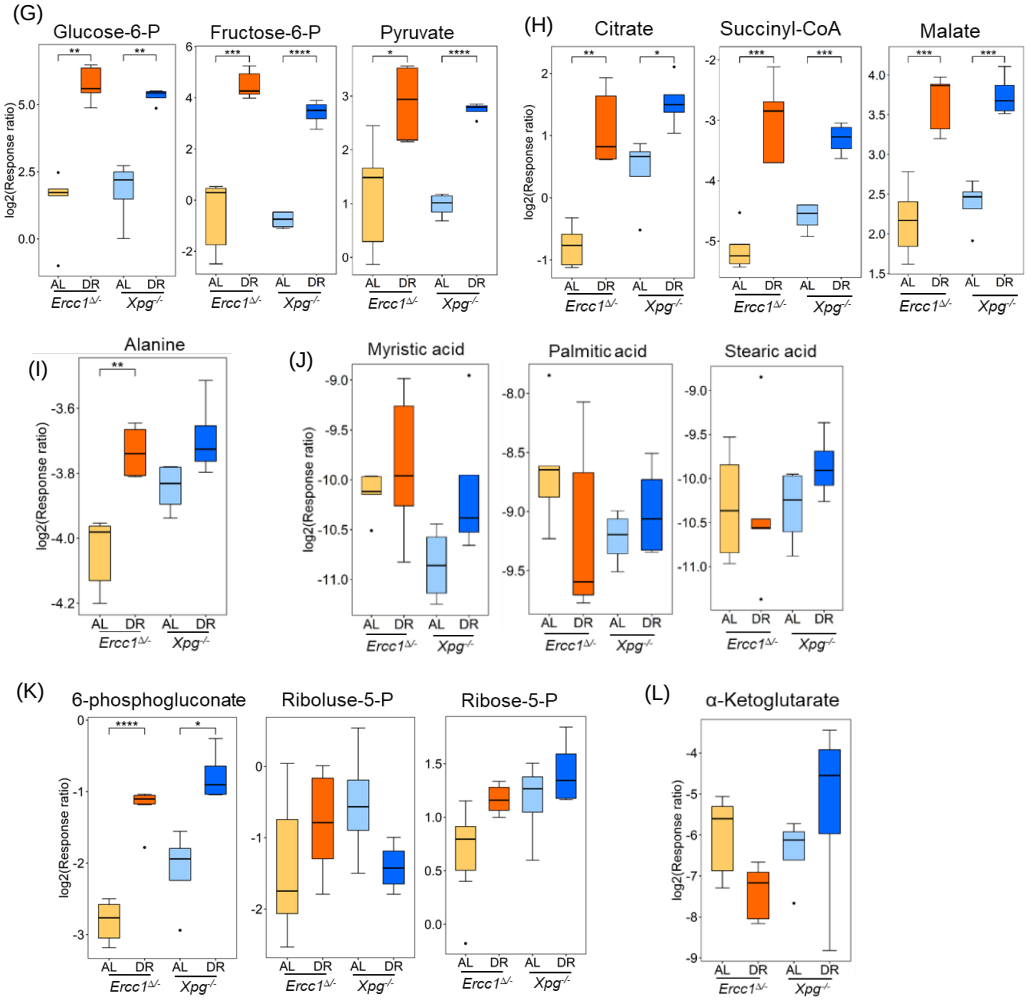

Figure 5. Footprint of the effects of DR on energy generation related metabolites and pathways for sarcopenia in *WT* (n=9), *Ercc1*$^{\Delta/-}$ (n=5), and *Xpg*$^{-/-}$ (n=4) mice.

(A) The PLS-DA score plot for the effect of DR on energy generation related metabolites;

(B) The effects of DR on the ratio of ATP to ADP in *Ercc1*$^{\Delta/-}$ and *Xpg*$^{-/-}$ mouse muscle. *p < 0.05, t test with FDR correction.;

(C) Heatmap profile of the energy generation related metabolites between AL and DR in *Ercc1*$^{\Delta/-}$ and *Xpg*$^{-/-}$ mouse muscle;

(D) The fold change of metabolites significantly (p<0.05) regulated in the energy generation related pathways (t test with FDR correction);

The effects of DR on (E) phosphocreatine to creatine, (F) energy substrates (*i.e.*, glucose in muscle and blood, and glucose-1-phosphate in muscle), (G) metabolites in glycolysis, (H) metabolites in Tricarboxylic Acid Cycle, (I) metabolite that stimulating gluconeogenesis, (J) saturated fatty acids, and (K) metabolites in pentose phosphate pathway (PPP), and (L) α-ketoglutarate in *Ercc1*$^{\Delta/-}$ and *Xpg*$^{-/-}$ mouse muscle. *p < 0.05, **p < 0.01, ***p < 0.001, ****p < 0.0001, t test with FDR correction.

Energy production in muscle tissue is highly related to grip strength and muscle function [76]. To determine the DR effects on muscle energy generation in sarcopenia, the related metabolites of glycolysis, tricarboxylic acid (TCA) cycle, gluconeogenesis, and saturated fatty acids (SFAs) lipolysis, were all analyzed. A clear segregation between AL and DR was observed in *Ercc1*$^{\Delta/-}$ and *Xpg*$^{-/-}$ mice (Figure 5A), indicating high modulation of energy-production-related metabolites by DR in the muscle of progeroid mice. Significantly ($p<0.05$) increased ATP/ADP ratio demonstrated improved energy status by DR in *Ercc1*$^{\Delta/-}$ and *Xpg*$^{-/-}$ mice (Figure 5B). The influence of fasting on the ATP/ADP ratio and energy status was minimized by sacrificing mice and collecting muscle samples 1-3.5 hours after feeding, when mice had just finished or were finishing their food intake. Phosphocreatine is considered as the "energy pool" in muscle cells and is preferentially consumed by generating creatine in case of an insufficient energy supply [77]. A heatmap profile of all analyzed energy-production and storage-related metabolites (Table S5) showed that most of the analytes were highly upregulated by DR (Figure 5C). To profile the DR effects, the fold change (Equation 2) of significantly ($p<0.05$) modulated metabolites in the main energy generation pathways, *i.e.*, glycolysis and TCA, and metabolites related to pentose phosphate pathway (PPP), gluconeogenesis, SFAs lipolysis, and phosphocreatine were shown in their pathways in Figure 5D. The significantly increased fold change of key metabolites in glycolysis and TCA cycle indicated upregulation of energy production and storage pathways by DR in *Ercc1*$^{\Delta/-}$ and *Xpg*$^{-/-}$ mice.

Phosphocreatine is generated from creatine by receiving a high-energy phosphate group split from ATP [77], therefore higher ratio value of phosphocreatine to creatine represents a higher energy status of muscle tissue. The significantly ($p<0.05$) increased ratio of phosphocreatine to creatine revealed that the energy status of muscle was notably improved by DR in *Ercc1*$^{\Delta/-}$ and *Xpg*$^{-/-}$ mice (Figure 5E), which may contribute to maintained grip strength and improved motor coordination by DR (Figure 1). Glycogen,

primarily in liver and muscle cells, is an important source to maintain energy balance. Fasting and DR can stimulate the transformation of liver and muscle glycogen to glucose and glucose-1-phosphate (glucose-1-P), respectively, to feed into glycolysis for energy production. The significantly ($p<0.001$) increased glucose-1-P in muscle tissue demonstrated the high consumption of muscle glycogen during DR (Figure 5F). Muscle consumes nearly 80% of the body's glucose content [78, 79]. The significantly ($p<0.01$) upregulated glucose levels in muscle indicated that glucose was transported from blood to muscle tissue because of DR (Figure 5F). The decreased blood glucose content by DR (Figure 4F) is consistent with earlier data [21]. This inverse glucose modulation in muscle and blood by DR may be due to the higher absorption of glucose in muscle tissue from blood after DR. The consumption of liver and muscle glycogen may also relate to the decreased mouse body weight in Figure 1A. Notably ($p<0.05$) increased glycose-6-phosphate (glycose-6-P), fructose-6-phosphate (fructose-6-P), and pyruvate by DR revealed significantly upregulated glycolysis by DR in progeroid mice (Figure 5G). Similarly, the notable ($p<0.05$) increased citrate, succinyl-CoA, and malate indicated a significant upregulation of TCA by DR in progeroid mice (Figure 5H).

Alanine was reported to be able to enhance gluconeogenesis in starvation [80]. Significantly ($p<0.01$) increased alanine also revealed upregulated gluconeogenesis by DR in muscle of progeroid mice (Figure 5I). SFAs are another potential energy source during DR. To profile the effects of DR on muscle energy generation pathways, three important SFAs, *i.e.*, myristic acid, palmitic acid, and stearic acid, were determined in *Ercc1*$^{\Delta/-}$ and *Xpg*$^{-/-}$ mouse muscle specimens. The results showed that all these SFAs were unaffected by DR (Figure 5J), indicating that DR did not induce lipolysis of SFAs in progeroid mice. Hence, the increased energy should originate from glycolysis, TCA, and gluconeogenesis from glycogen.

The significantly ($p<0.05$) increase of 6-phosphogluconate by DR may be due to the elevated level of its precursor glucose-6-P (Figure 5K). Ribose 5-phosphate (ribose-5-P) is the source for the synthesis of nucleotides [81]. The unaffected ribose-5-P and ribulose-5-phosphate (ribulose 5-P) levels by DR (Figure 5K) indicated that these precursors of nucleotides synthesis were not accumulating consistent with the general suppression of growth and enhanced salvage pathways by DR. In summary, this extensive metabolic analysis revealed key changes in sarcopenic muscle of prematurely aging repair-deficient

mice and strong improvements in oxidative stress, anti-inflammation, and energy status upon calorie restriction, which help explaining the preservation of muscle function induced by DR.

4. Discussion

In this study we performed a metabolomic analysis of the quadriceps muscle of progeroid DNA repair mouse lines that dietary restriction (DR) effects on sarcopenia. Our data showed that DR significantly decreased body weight and improved motor learning and coordination performance in our repair-deficient progeroid mice, consistent with studies in naturally aged mice [82]. Analysis of key energy metabolites showed that DR-treated animals at the moment of sacrifice exhibited enhanced conversion of liver and muscle glycogen to glucose and glucose-1-P, respectively, to feed into glycolysis in muscle, and simultaneously upregulated other pathways of gluconeogenesis. This might at least in part be due to the short time between feeding and harvesting of the animals. The increased energy resources enabled upregulation of glycolysis and TCA in muscle, which improved energy production and storage in phosphocreatine (Figure 6). Similar observations were reported by Xie *et al*., who found that caloric restriction increases energy production and supply for muscle exercise, and significantly improves muscle work efficiency [79]. The further increased energy status by DR, *i.e*., ATP/ADP ratio (Figure 5B), may be due to the upregulation of the two major energy generation pathways, glycolysis, and TCA, which is distinct from the reduced consumption of ATP in AL-fed *Ercc1*$^{\Delta/-}$ and *Xpg*$^{-/-}$ mice (Figure 2D). The improved energy metabolism by DR may be enabled by the lower DNA damage induced transcription stress [21, 33], leading to improved gene expression output. Conversely, the metabolic redesign brought about by DR may lower the endogenously generated DNA damage load and thereby diminish the transcription stress, caused by transcription-stalling DNA lesions [21, 50]. Importantly, the occurrence of DNA-damage-induced transcription stress in natural aging [33] supports a similar scenario in physiological situations of age-associated sarcopenia. Interestingly, elevated glycolysis and TCA would additionally infer an increase of the downstream metabolite α-ketoglutarate (aKG), a metabolite recently implicated in extension of lifespan and compression of morbidity [83]. Indeed, aKG was elevated locally in *Xpg*$^{-/-}$ muscle upon DR (Figure 5L), opening opportunities for further research in both models for assessing and modulating aKG levels locally and systemically, potentially also for counteracting accelerated aging and sarcopenia [39].

Polyunsaturated fatty acids (PUFAs) are among the most oxygen-sensitive components in nature and were reported as the main generator of superoxide by the reaction of lipoxygenases catalyzed by metal ions, in particular iron ions [84]. LA is the main PUFA in most diets, typically consumed in 5- to 20-fold greater amounts than ALA [85], and around 8.4-fold larger amounts than ALA in synthetic AIN93G chow, the food provided to the mice in this study [86]. DR significantly reduced the supply of these two essential PUFAs, LA and ALA, leading to their downregulation in *Ercc1*$^{\Delta/-}$ and *Xpg*$^{-/-}$ mouse muscle. DR also contributes to the lower iron accumulation in skeletal muscle [87]. Both, the decreased LA content and reduced iron accumulation may at least in part account for the lower level of oxidative stress in progeroid mouse muscle (Figure 6), as apparent from the downregulation of oxidative stress indicators, *i.e.*, 9-HODE, 12(S)-HHTrE and 11-HETE, and may contribute to diminished adverse effects for muscle cell/tissue function (Figure 6). Similar results of down-modulated oxidative stress mediators by DR or caloric restriction were also previously reported in normal aging and in man [24, 25]. Simultaneously, decreased LA induced down-modulation of its downstream ω6 PUFAs, *i.e.*, GLA, DGLA, and AA, which further contributed to the lower generation of other pro-inflammatory mediators, *i.e.*, PGE_2, PGD_2, TXB_2, and 11-HETE, and stimulation of muscle growth by $PGF_{2\alpha}$. The reduced pro-inflammation by caloric restriction is in line with literature of physiological aging, stressing the parallels between accelerated and natural aging and the anti-aging effect of DR [66, 88, 89].

Interestingly, even though there is a significant decrease of DGLA and AA, their downstream anti-inflammatory products, *i.e.*, PGF_1 and 8,9-EET, were notably increased by DR (Figure 6). ALA and its downstream ω3 PUFAs, *i.e.*, EPA, DPA and DHA, were also notably reduced by DR, however, some anti-inflammatory mediators generated from EPA and ALA, *i.e.*, 14,15-DiHETE and 12,13-DiHODE, were significantly upregulated by DR. The enhanced anti-inflammatory mediators by caloric restriction, including β-hydroxybutyrate, were also reported by González *et al*. [66] and Carlos *et al*. [17]. John *et al*. observed a strong correlation between increased β-hydroxybutyrate concentration and reduced mortality (and improved memory) in aging mice with ketogenic diet [90].

The upregulated anti-inflammatory and downregulated pro-inflammatory mediators resulted in lower chronic inflammation in the progeroid mice, which in combination with the lower oxidative stress, and lower energy expenditure contributed to improved muscle

quality and performance (Figure 6) [91-93]. Similar results of reduced energy costs and ROS production by DR in humans were also reported by Heilbronn *et al*. [23], Almundarij *et al*. [26], and Civitarese *et al*. [94].

It is important to note that DNA-repair-deficient *Ercc1*$^{\Delta/-}$ mice are extremely sensitive to dietary PUFAs and live shorter when administered a high PUFA diet [51]. This suggests that PUFAs elevate endogenous DNA damage, potentially via iron-dependent lipid peroxidation [51, 95] and aldehyde formation enhancing DNA-damage-induced transcription stress [33, 96, 97]. Reducing endogenous metabolites with DNA-damaging capacities, like PUFA, and potentially downstream aldehydes, could contribute to the mechanism of action by which DR lowers transcription stress and results in such an enormous life- and health span extending effect in *Ercc1*$^{\Delta/-}$ and *Xpg*$^{-/-}$ mice [21]. Enhanced energy production, lower energy expenditure, and reduced DNA damage and consequent transcription stress by DR likely all contribute to the dramatically extended health- and lifespan of progeroid mouse, including improved muscle quality, unaffected grip strength and improved motor coordination and learning performance by DR in *Ercc1*$^{\Delta/-}$ and *Xpg*$^{-/-}$ mice. This comprehensive analysis provides fundamental metabolomics insight into the anti-aging effects of DR on sarcopenia and represents a snapshot in the progressive development of the premature aging phenotype, in fact at a relatively late stage. In the future it may be interesting to compare this also to early stages to better understand the various intermediate steps leading to the development of sarcopenia. Further multi-omics studies including transcriptomics (in relation with transcription stress) and proteomics (in combination with systemic circulating changes) to investigate the DR effects on muscle proteins and function may provide a more complete reference framework for future clinical therapy of sarcopenia.

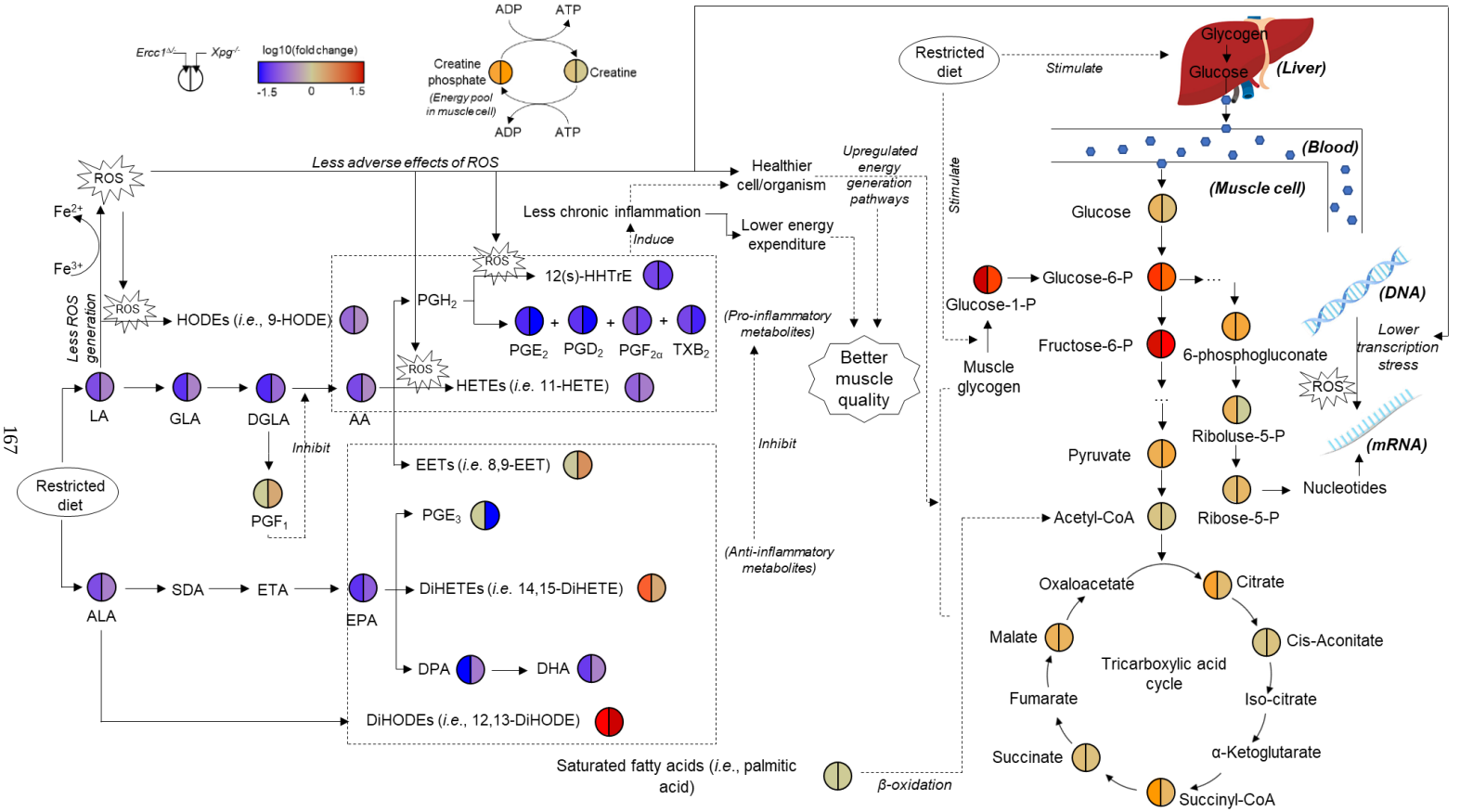

Figure 6. Overview of the metabolites and pathways regulated by DR to improve muscle quality and function in sarcopenia in DNA-repair-deficient prematurely aging mouse mutants.

5. Conclusion

Dietary restriction (DR) decreased the mouse body weight, however, the forelimbs and all limbs grip strength were unaffected, and rotarod motor coordination and learning performance was significantly improved by DR in *WT*, *Ercc1*$^{\Delta/-}$, and *Xpg*$^{-/-}$ mice. The decreased mouse body weight may be related to the downregulated muscle growth stimulation metabolite ($PGF_{2\alpha}$) and the improved consumption of muscle and liver glycogen by DR. Simultaneously, DR may improve the muscle quality and function by downregulating oxidative stress and pro-inflammatory mediators, upregulating anti-inflammatory mediators, up-modulating energy production pathways, and reducing transcription stress in *Ercc1*$^{\Delta/-}$ and *Xpg*$^{-/-}$ mice.

This study provided a fundamental metabolomics mechanism insight of the DR effects on sarcopenia. Further multi-omics study, *i.e.*, transcriptomics and proteomics, could be utilized to investigate the DR effects on muscle enzymes and proteins, to identify not only metabolite biomarkers, but also the potential protein biomarkers for sarcopenia, and may provide more reference information for the future clinical therapy of sarcopenia.

Acknowledgements

Funding: This work was supported by the Netherlands Organisation for Scientific Research (NWO) in the Building Blocks of Life program [grant number 737.016.015] and the China Scholarship Council (CSC) [No. 201706320322]. JH was additionally supported by the European Research Council Advanced Grant Dam2Age, NIH grant (PO1 AG017242), the Deutsche Forschungsgemeinschaft – Project-ID 73111208 – SFB 829, JH and WV by EJP-RD TC-NER RD20-113, DJ, JH and WV by ZonMW Memorabel (733050810), and YR, KS, JH, and WV ONCODE (Dutch Cancer Society). This research was (partially) funded by X-Omics (NWO, project 184.034.019) and by the Medical Delta program METABODELTA.

Reference

[1] V. Santilli, A. Bernetti, M. Mangone, and M. Paoloni, Clinical definition of sarcopenia. Clinical cases in mineral and bone metabolism : the official journal of the Italian Society of Osteoporosis, Mineral Metabolism, and Skeletal Diseases, (11) 2014. 177-180.

[2] R.A. Fielding, B. Vellas, W.J. Evans, S. Bhasin, J.E. Morley, A.B. Newman, G. Abellan van Kan, S. Andrieu, J. Bauer, D. Breuille, T. Cederholm, J. Chandler, C. De Meynard, L. Donini, T. Harris, A. Kannt, F. Keime Guibert, G. Onder, D. Papanicolaou, Y. Rolland, D. Rooks, C. Sieber, E. Souhami, S. Verlaan, and M. Zamboni, Sarcopenia: an undiagnosed condition in older adults. Current consensus definition: prevalence, etiology, and consequences. International working group on sarcopenia. J Am Med Dir Assoc, (12) 2011. 249-56.

[3] N. Garatachea, H. Pareja-Galeano, F. Sanchis-Gomar, A. Santos-Lozano, C. Fiuza-Luces, M. Moran, E. Emanuele, M.J. Joyner, and A. Lucia, Exercise attenuates the major hallmarks of aging. Rejuvenation Res, (18) 2015. 57-89.

[4] S. von Haehling, J.E. Morley, and S.D. Anker, An overview of sarcopenia: facts and numbers on prevalence and clinical impact. J Cachexia Sarcopenia Muscle, (1) 2010. 129-133.

[5] X. Dong, B. Milholland, and J. Vijg, Evidence for a limit to human lifespan. Nature, (538) 2016. 257-259.

[6] L. Partridge, J. Deelen, and P.E. Slagboom, Facing up to the global challenges of ageing. Nature, (561) 2018. 45-56.

[7] J.Y. Kwak and K.-S. Kwon, Pharmacological Interventions for Treatment of Sarcopenia: Current Status of Drug Development for Sarcopenia. Annals of geriatric medicine and research, (23) 2019. 98-104.

[8] C.G.S. Rosa, J.R. Colares, S.R.B. da Fonseca, G.d.S. Martins, F.M. Miguel, A.S. Dias, C.A. Marroni, J.N. Picada, M. Lehmann, and N.A.P. Marroni, Sarcopenia, oxidative stress and inflammatory process in muscle of cirrhotic rats – Action of melatonin and physical exercise. Experimental and Molecular Pathology, (121) 2021. 104662.

[9] S.-J. Meng and L.-J. Yu, Oxidative stress, molecular inflammation and sarcopenia. International journal of molecular sciences, (11) 2010. 1509-1526.

[10] F. Bellanti, A.L. Buglio, and G. Vendemiale, Chapter 9 - Oxidative stress and sarcopenia, in Aging (Second Edition), V.R. Preedy and V.B. Patel, Editors. 2020, Academic Press. p. 95-103.

[11] C. Howard, L. Ferrucci, K. Sun, L.P. Fried, J. Walston, R. Varadhan, J.M. Guralnik, and R.D. Semba, Oxidative protein damage is associated with poor grip strength among older women living in the community. Journal of applied physiology (Bethesda, Md. : 1985), (103) 2007. 17-20.

[12] O. Pastoris, F. Boschi, M. Verri, P. Baiardi, G. Felzani, J. Vecchiet, M. Dossena, and M. Catapano, The effects of aging on enzyme activities and metabolite concentrations in skeletal muscle from sedentary male and female subjects. Exp Gerontol, (35) 2000. 95-104.

[13] K.S. Nair, Aging muscle. American Journal of Clinical Nutrition, (81) 2005. 953-963.

[14] B.S. Kirby, A.R. Crecelius, W.F. Voyles, and F.A. Dinenno, Impaired Skeletal Muscle Blood Flow Control With Advancing Age in Humans Attenuated ATP Release and Local Vasodilation During Erythrocyte Deoxygenation. Circulation Research, (111) 2012. 220-U245.

[15] S. Fujita and E. Volpi, Amino acids and muscle loss with aging. Journal of Nutrition, (136) 2006. 277s-280s.

[16] M. Sheffield-Moore, D. Paddon-Jones, and R.J. Urban, Amino acid supplementation and skeletal muscle metabolism in ageing populations. Hormone Research, (66) 2006. 93-97.

[17] C. López-Otín, L. Galluzzi, J.M.P. Freije, F. Madeo, and G. Kroemer, Metabolic Control of Longevity. Cell, (166) 2016. 802-821.

[18] R.S. Sohal and R. Weindruch, Oxidative stress, caloric restriction, and aging. Science, (273) 1996. 59-63.

[19] R. Weindruch, R.L. Walford, S. Fligiel, and D. Guthrie, The retardation of aging in mice by dietary restriction: longevity, cancer, immunity and lifetime energy intake. J Nutr, (116) 1986. 641-54.

[20] A. Chaix, T. Lin, H.D. Le, M.W. Chang, and S. Panda, Time-Restricted Feeding Prevents Obesity and Metabolic Syndrome in Mice Lacking a Circadian Clock. Cell Metabolism, (29) 2019. 303-319.e4.
[21] W.P. Vermeij, M.E.T. Dollé, E. Reiling, D. Jaarsma, C. Payan-Gomez, C.R. Bombardieri, H. Wu, A.J.M. Roks, S.M. Botter, B.C. van der Eerden, S.A. Youssef, R.V. Kuiper, B. Nagarajah, C.T. van Oostrom, R.M.C. Brandt, S. Barnhoorn, S. Imholz, J.L.A. Pennings, A. de Bruin, Á. Gyenis, J. Pothof, J. Vijg, H. van Steeg, and J.H.J. Hoeijmakers, Restricted diet delays accelerated ageing and genomic stress in DNA-repair-deficient mice. Nature, (537) 2016. 427-431.
[22] R.J. Colman, T.M. Beasley, D.B. Allison, and R. Weindruch, Attenuation of sarcopenia by dietary restriction in rhesus monkeys. The journals of gerontology. Series A, Biological sciences and medical sciences, (63) 2008. 556-559.
[23] L.K. Heilbronn, L. de Jonge, M.I. Frisard, J.P. DeLany, D.E. Larson-Meyer, J. Rood, T. Nguyen, C.K. Martin, J. Volaufova, M.M. Most, F.L. Greenway, S.R. Smith, W.A. Deutsch, D.A. Williamson, E. Ravussin, and C.T. Pennington, Effect of 6-month calorie restriction on biomarkers of longevity, metabolic adaptation, and oxidative stress in overweight individuals: a randomized controlled trial. JAMA, (295) 2006. 1539-48.
[24] L.M. Redman, S.R. Smith, J.H. Burton, C.K. Martin, D. Il'yasova, and E. Ravussin, Metabolic Slowing and Reduced Oxidative Damage with Sustained Caloric Restriction Support the Rate of Living and Oxidative Damage Theories of Aging. Cell Metabolism, 2018.
[25] E.F. Sutton, R. Beyl, K.S. Early, W.T. Cefalu, E. Ravussin, and C.M. Peterson, Early Time-Restricted Feeding Improves Insulin Sensitivity, Blood Pressure, and Oxidative Stress Even without Weight Loss in Men with Prediabetes. Cell Metabolism, (27) 2018. 1212-1221.e3.
[26] T.I. Almundarij, C.K. Gavini, and C.M. Novak, Suppressed sympathetic outflow to skeletal muscle, muscle thermogenesis, and activity energy expenditure with calorie restriction. Physiological reports, (5) 2017. e13171.
[27] G. Valdez, J.C. Tapia, H. Kang, G.D. Clemenson, Jr., F.H. Gage, J.W. Lichtman, and J.R. Sanes, Attenuation of age-related changes in mouse neuromuscular synapses by caloric restriction and exercise. Proc Natl Acad Sci U S A, (107) 2010. 14863-8.
[28] Y.C. Jang, Y. Liu, C.R. Hayworth, A. Bhattacharya, M.S. Lustgarten, F.L. Muller, A. Chaudhuri, W. Qi, Y. Li, J.Y. Huang, E. Verdin, A. Richardson, and H. Van Remmen, Dietary restriction attenuates age-associated muscle atrophy by lowering oxidative stress in mice even in complete absence of CuZnSOD. Aging Cell, (11) 2012. 770-82.
[29] C. López-Otín, M.A. Blasco, L. Partridge, M. Serrano, and G. Kroemer, The hallmarks of aging. Cell, (153) 2013. 1194-1217.
[30] B. Schumacher, J. Pothof, J. Vijg, and J.H.J. Hoeijmakers, The central role of DNA damage in the ageing process. Nature, (592) 2021. 695-703.
[31] W.M. van den Boogaard, M.M. van den Heuvel-Eibrink, J.H. Hoeijmakers, and W.P. Vermeij, Nutritional preconditioning in cancer treatment in relation to DNA damage and aging. Annual Review of Cancer Biology, (5) 2021. 161-179.
[32] L.J. Niedernhofer, A.U. Gurkar, Y. Wang, J. Vijg, J.H.J. Hoeijmakers, and P.D. Robbins, Nuclear Genomic Instability and Aging. Annu Rev Biochem, (87) 2018. 295-322.
[33] A. Gyenis, J. Chang, J.J.P.G. Demmers, S.T. Bruens, S. Barnhoorn, R. Brandt, M.P. Baar, M. Raseta, K.W.J. Derks, J.H.J. Hoeijmakers, and J. Pothof, Genome-wide transcription stalling by DNA damage shapes the transcriptome in aging. Nature Genetics, 2022. In press.
[34] H. Lans, J.H.J. Hoeijmakers, W. Vermeulen, and J.A. Marteijn, The DNA damage response to transcription stress. Nature Reviews Molecular Cell Biology, (20) 2019. 766-784.
[35] W.P. Vermeij, J.H. Hoeijmakers, and J. Pothof, Genome Integrity in Aging: Human Syndromes, Mouse Models, and Therapeutic Options. Annu Rev Pharmacol Toxicol, (56) 2016. 427-45.
[36] L.J. Niedernhofer, G.A. Garinis, A. Raams, A.S. Lalai, A.R. Robinson, E. Appeldoorn, H. Odijk, R. Oostendorp, A. Ahmad, and W. Van Leeuwen, A new progeroid syndrome reveals that genotoxic stress suppresses the somatotroph axis. Nature, (444) 2006. 1038-1043.

[37] M.E. Dollé, R.V. Kuiper, M. Roodbergen, J. Robinson, S. de Vlugt, S.W. Wijnhoven, R.B. Beems, L. de la Fonteyne, P. de With, and I. van der Pluijm, Broad segmental progeroid changes in short-lived Ercc1−/Δ7 mice. Pathobiology of Aging & Age-related Diseases, (1) 2011. 7219.

[38] S. Barnhoorn, L.M. Uittenboogaard, D. Jaarsma, W.P. Vermeij, M. Tresini, M. Weymaere, H. Menoni, R.M. Brandt, M.C. de Waard, S.M. Botter, A.H. Sarker, N.G. Jaspers, G.T. van der Horst, P.K. Cooper, J.H. Hoeijmakers, and I. van der Pluijm, Cell-autonomous progeroid changes in conditional mouse models for repair endonuclease XPG deficiency. PLoS Genet, (10) 2014. e1004686.

[39] K. Alyodawi, W.P. Vermeij, S. Omairi, O. Kretz, M. Hopkinson, F. Solagna, B. Joch, R.M.C. Brandt, S. Barnhoorn, N. van Vliet, Y. Ridwan, J. Essers, R. Mitchell, T. Morash, A. Pasternack, O. Ritvos, A. Matsakas, H. Collins-Hooper, T.B. Huber, J.H.J. Hoeijmakers, and K. Patel, Compression of morbidity in a progeroid mouse model through the attenuation of myostatin/activin signalling. J Cachexia Sarcopenia Muscle, (10) 2019. 662-686.

[40] A. Zhang, H. Sun, G. Yan, P. Wang, and X. Wang, Metabolomics for Biomarker Discovery: Moving to the Clinic. BioMed research international, (2015) 2015. 354671-354671.

[41] G. Weeda, I. Donker, J. de Wit, H. Morreau, R. Janssens, C.J. Vissers, A. Nigg, H. van Steeg, D. Bootsma, and J.H. Hoeijmakers, Disruption of mouse ERCC1 results in a novel repair syndrome with growth failure, nuclear abnormalities and senescence. Curr Biol, (7) 1997. 427-39.

[42] Y. He, M. van Mever, W. Yang, L. Huang, R. Ramautar, Y. Rijksen, W.P. Vermeij, J.H. Hoeijmakers, A.C. Harms, and P.W. Lindenburg, A Sample Preparation Method for the Simultaneous Profiling of Signaling Lipids and Polar Metabolites in Small Quantities of Muscle Tissues from a Mouse Model for Sarcopenia. Metabolites, (12) 2022. 742.

[43] A. Di Zazzo, W. Yang, M. Coassin, A. Micera, M. Antonini, F. Piccinni, M. De Piano, I. Kohler, A.C. Harms, T. Hankemeier, S. Boinini, and A. Mashaghi, Signaling lipids as diagnostic biomarkers for ocular surface cicatrizing conjunctivitis. Journal of Molecular Medicine-Jmm, (98) 2020. 751-760.

[44] F. Hosseinkhani, L. Huang, A.-C. Dubbelman, F. Guled, A.C. Harms, and T. Hankemeier, Systematic Evaluation of HILIC Stationary Phases for Global Metabolomics of Human Plasma. Metabolites, (12) 2022. 165.

[45] M.E.T. Dollé, R.V. Kuiper, M. Roodbergen, J. Robinson, S. de Vlugt, S.W.P. Wijnhoven, R.B. Beems, L. de la Fonteyne, P. de With, I. van der Pluijm, L.J. Niedernhofer, P. Hasty, J. Vijg, J.H.J. Hoeijmakers, and H. van Steeg, Broad segmental progeroid changes in short-lived Ercc1(-/Δ7) mice. Pathobiology of aging & age related diseases, (1) 2011. 10.3402/pba.v1i0.7219.

[46] J.F. Gill, G. Santos, S. Schnyder, and C. Handschin, PGC-1α affects aging-related changes in muscle and motor function by modulating specific exercise-mediated changes in old mice. Aging cell, (17) 2018. e12697.

[47] O. Zitka, S. Skalickova, J. Gumulec, M. Masarik, V. Adam, J. Hubalek, L. Trnkova, J. Kruseova, T. Eckschlager, and R. Kizek, Redox status expressed as GSH: GSSG ratio as a marker for oxidative stress in paediatric tumour patients. Oncology letters, (4) 2012. 1247-1253.

[48] L. Wang, P. Chen, and W. Xiao, β-hydroxybutyrate as an Anti-Aging Metabolite. Nutrients, (13) 2021. 3420.

[49] J.-S. Park and Y.-J. Kim, Anti-Aging Effect of the Ketone Metabolite β-Hydroxybutyrate in Drosophila Intestinal Stem Cells. International Journal of Molecular Sciences, (21) 2020. 3497.

[50] C. Milanese, C.R. Bombardieri, S. Sepe, S. Barnhoorn, C. Payán-Goméz, D. Caruso, M. Audano, S. Pedretti, W.P. Vermeij, R.M.C. Brandt, A. Gyenis, M.M. Wamelink, A.S. de Wit, R.C. Janssens, R. Leen, A.B.P. van Kuilenburg, N. Mitro, J.H.J. Hoeijmakers, and P.G. Mastroberardino, DNA damage and transcription stress cause ATP-mediated redesign of metabolism and potentiation of anti-oxidant buffering. Nat Commun, (10) 2019. 4887.

[51] J. Czerwińska, M. Nowak, P. Wojtczak, D. Dziuban-Lech, J.M. Cieśla, D. Kołata, B. Gajewska, A. Barańczyk-Kuźma, A.R. Robinson, H.L. Shane, S.Q. Gregg, L.H. Rigatti, M.J. Yousefzadeh, A.U. Gurkar, S.J. McGowan, K. Kosicki, M. Bednarek, E. Zarakowska, D. Gackowski, R. Oliński, E. Speina, L.J. Niedernhofer, and B. Tudek, ERCC1-deficient cells and mice are hypersensitive to lipid peroxidation. Free Radic Biol Med, (124) 2018. 79-96.

[52] N. Kaur, V. Chugh, and A.K. Gupta, Essential fatty acids as functional components of foods- a review. Journal of Food Science and Technology-Mysore, (51) 2014. 2289-2303.
[53] R.D. Gu, The role of prostaglandins in the inflammation and immunity of human palatine tonsils. Zhonghua Er Bi Yan Hou Ke Za Zhi, (28) 1993. 100-1, 124-5.
[54] J.K. Kiecolt-Glaser, Stress, Food, and Inflammation: Psychoneuroimmunology and Nutrition at the Cutting Edge. Psychosomatic Medicine, (72) 2010. 365-369.
[55] V. Vangaveti, B.T. Baune, and R.L. Kennedy, Hydroxyoctadecadienoic acids: novel regulators of macrophage differentiation and atherogenesis. Ther Adv Endocrinol Metab, (1) 2010. 51-60.
[56] D.C. Nieman, M.P. Meaney, C.S. John, K.J. Knagge, and H. Chen, 9- and 13-Hydroxy-octadecadienoic acids (9+13 HODE) are inversely related to granulocyte colony stimulating factor and IL-6 in runners after 2h running. Brain, Behavior, and Immunity, (56) 2016. 246-252.
[57] T. Sumiya, Y. Fujimoto, H. Nishida, Y. Morikawa, S. Sakuma, and T. Fujita, Effects of reactive oxygen species on arachidonic acid metabolism in rabbit platelets. Free Radic Biol Med, (15) 1993. 101-4.
[58] H.G. Johnson, M.L. McNee, and F.F. Sun, 15-Hydroxyeicosatetraenoic acid is a potent inflammatory mediator and agonist of canine tracheal mucus secretion. Am Rev Respir Dis, (131) 1985. 917-22.
[59] C. Austin Pickens, Z. Yin, L.M. Sordillo, and J.I. Fenton, Arachidonic acid-derived hydroxyeicosatetraenoic acids are positively associated with colon polyps in adult males: a cross-sectional study. Scientific Reports, (9) 2019. 12033.
[60] M.G. Di Pasquale, The essentials of essential fatty acids. J Diet Suppl, (6) 2009. 143-61.
[61] J. Bézard, J.P. Blond, A. Bernard, and P. Clouet, The metabolism and availability of essential fatty acids in animal and human tissues. Reprod Nutr Dev, (34) 1994. 539-68.
[62] V. Horsley and G.K. Pavlath, Prostaglandin F2(alpha) stimulates growth of skeletal muscle cells via an NFATC2-dependent pathway. J Cell Biol, (161) 2003. 111-8.
[63] K.M. Jansen and G.K. Pavlath, Prostaglandin F2 α promotes muscle cell survival and growth through upregulation of the inhibitor of apoptosis protein BRUCE. Cell Death & Differentiation, (15) 2008. 1619-1628.
[64] B. Schumacher, I. van der Pluijm, M.J. Moorhouse, T. Kosteas, A.R. Robinson, Y. Suh, T.M. Breit, H. van Steeg, L.J. Niedernhofer, W. van Ijcken, A. Bartke, S.R. Spindler, J.H. Hoeijmakers, G.T. van der Horst, and G.A. Garinis, Delayed and accelerated aging share common longevity assurance mechanisms. PLoS Genet, (4) 2008. e1000161.
[65] T. Finkel, The metabolic regulation of aging. Nat Med, (21) 2015. 1416-23.
[66] O.A. González, C. Tobia, J.L. Ebersole, and M.J. Novak, Caloric restriction and chronic inflammatory diseases. Oral diseases, (18) 2012. 16-31.
[67] P.C. Calder, n-3 fatty acids and cardiovascular disease: evidence explained and mechanisms explored. Clinical Science, (107) 2004. 1-11.
[68] Y.Y. Fan and R.S. Chapkin, Importance of dietary gamma-linolenic acid in human health and nutrition. Journal of Nutrition, (128) 1998. 1411-1414.
[69] C. Morisseau and B.D. Hammock, Impact of soluble epoxide hydrolase and epoxyeicosanoids on human health. Annual review of pharmacology and toxicology, (53) 2013. 37-58.
[70] A. Saika, T. Nagatake, S.I. Hirata, K. Sawane, J. Adachi, Y. Abe, J. Isoyama, S. Morimoto, E. Node, P. Tiwari, K. Hosomi, A. Matsunaga, T. Honda, T. Tomonaga, M. Arita, K. Kabashima, and J. Kunisawa, omega3 fatty acid metabolite, 12-hydroxyeicosapentaenoic acid, alleviates contact hypersensitivity by downregulation of CXCL1 and CXCL2 gene expression in keratinocytes via retinoid X receptor alpha. FASEB J, (35) 2021. e21354.
[71] C.J. Wang, W.L. Liu, L. Yao, X.J. Zhang, X. Zhang, C.J. Ye, H.F. Jiang, J.L. He, Y. Zhu, and D. Ai, Hydroxyeicosapentaenoic acids and epoxyeicosatetraenoic acids attenuate early occurrence of nonalcoholic fatty liver disease. British Journal of Pharmacology, (174) 2017. 2358-2372.
[72] I. Vachier, P. Chanez, C. Bonnans, P. Godard, J. Bousquet, and C. Chavis, Endogenous anti-inflammatory mediators from arachidonate in human neutrophils. Biochem Biophys Res Commun, (290) 2002. 219-24.

[73] M. Svenvik, J. Raffetseder, L. Brudin, R. Lindberg, M. Blomberg, D. Axelsson, M.C. Jenmalm, J. Ernerudh, and M.L. Nording, Plasma oxylipin levels associated with preterm birth in preterm labor☆. Prostaglandins, Leukotrienes and Essential Fatty Acids, (166) 2021. 102251.
[74] J. Xu, Y. Yuan, Y.-Y. Chen, C.-F. Xiong, Z. Zhang, and Y.-Q. Feng, Carboxylic submetabolome-driven signature characterization of COVID-19 asymptomatic infection. Talanta, (239) 2022. 123086.
[75] K. Aquilano, S. Baldelli, and M.R. Ciriolo, Glutathione: new roles in redox signaling for an old antioxidant. Frontiers in pharmacology, (5) 2014. 196.
[76] K. Norman, N. Stobäus, H. Lochs, and M. Pirlich, Measurement of hand grip strength as nutritional outcome parameter. Aktuelle Ernährungsmedizin, (34) 2009. 263-268.
[77] R.A. Rhoades and D.R. Bell, Medical phisiology: Principles for clinical medicine. 2012: Lippincott Williams & Wilkins.
[78] R.A. DeFronzo and D. Tripathy, Skeletal muscle insulin resistance is the primary defect in type 2 diabetes. Diabetes care, (32 Suppl 2) 2009. S157-S163.
[79] W.-Q. Xie, W.-F. Xiao, K. Tang, Y.-X. Wu, P.-W. Hu, Y.-S. Li, Y. Duan, and S. Lv, Caloric restriction: implications for sarcopenia and potential mechanisms. Aging, (12) 2020. 24441-24452.
[80] J.G. Salway, Metabolism at a Glance. 2016: John Wiley & Sons.
[81] G.D. Khedkar, B. Prakash, C.D. Khedkar, and B.A. Chopade, Nucleic Acids, in Encyclopedia of Food and Health, B. Caballero, P.M. Finglas, and F. Toldrá, Editors. 2016, Academic Press: Oxford. p. 84-92.
[82] D.K. Ingram, R. Weindruch, E.L. Spangler, J.R. Freeman, and R.L. Walford, Dietary Restriction Benefits Learning and Motor Performance of Aged Mice. Journal of Gerontology, (42) 1987. 78-81.
[83] A. Asadi Shahmirzadi, D. Edgar, C.Y. Liao, Y.M. Hsu, M. Lucanic, A. Asadi Shahmirzadi, C.D. Wiley, G. Gan, D.E. Kim, H.G. Kasler, C. Kuehnemann, B. Kaplowitz, D. Bhaumik, R.R. Riley, B.K. Kennedy, and G.J. Lithgow, Alpha-Ketoglutarate, an Endogenous Metabolite, Extends Lifespan and Compresses Morbidity in Aging Mice. Cell Metab, (32) 2020. 447-456.e6.
[84] G. Spiteller, Is Lipid Peroxidation of Polyunsaturated Acids the Only Source of Free Radicals That Induce Aging and Age-Related Diseases? Rejuvenation Research, (13) 2010. 91-103.
[85] M. Macsai and G. Mojica, 34 - Medical Management of Ocular Surface Disease, in Ocular Surface Disease: Cornea, Conjunctiva and Tear Film, E.J. Holland, M.J. Mannis, and W.B. Lee, Editors. 2013, W.B. Saunders: London. p. 271-281.
[86] A.P. Kitson, T.L. Smith, K.A. Marks, and K.D. Stark, Tissue-specific sex differences in docosahexaenoic acid and Delta6-desaturase in rats fed a standard chow diet. Appl Physiol Nutr Metab, (37) 2012. 1200-11.
[87] T. Hofer, E. Marzetti, J. Xu, A.Y. Seo, S. Gulec, M.D. Knutson, C. Leeuwenburgh, and E.E. Dupont-Versteegden, Increased iron content and RNA oxidative damage in skeletal muscle with aging and disuse atrophy. Experimental gerontology, (43) 2008. 563-570.
[88] S. Ma, S. Sun, L. Geng, M. Song, W. Wang, Y. Ye, Q. Ji, Z. Zou, S. Wang, X. He, W. Li, C.R. Esteban, X. Long, G. Guo, P. Chan, Q. Zhou, J.C.I. Belmonte, W. Zhang, J. Qu, and G.-H. Liu, Caloric Restriction Reprograms the Single-Cell Transcriptional Landscape of Rattus Norvegicus Aging. Cell, (180) 2020. 984-1001.e22.
[89] H.R. Lijnen, M. Van Hul, and B. Hemmeryckx, Caloric restriction improves coagulation and inflammation profile in obese mice. Thromb Res, (129) 2012. 74-9.
[90] J.C. Newman, A.J. Covarrubias, M. Zhao, X. Yu, P. Gut, C.-P. Ng, Y. Huang, S. Haldar, and E. Verdin, Ketogenic Diet Reduces Midlife Mortality and Improves Memory in Aging Mice. Cell Metabolism, (26) 2017. 547-557.e8.
[91] H. Wang and J. Ye, Regulation of energy balance by inflammation: common theme in physiology and pathology. Rev Endocr Metab Disord, (16) 2015. 47-54.
[92] A.A. Floh, M. Nakada, G. La Rotta, K. Mah, J.E. Herridge, G. Van Arsdell, and S.M. Schwartz, Systemic Inflammation Increases Energy Expenditure Following Pediatric Cardiopulmonary Bypass. Pediatric Critical Care Medicine, (16) 2015. 343-351.

[93] M. He, A.C. Harms, E. van Wijk, M. Wang, R. Berger, S. Koval, T. Hankemeier, and J. van der Greef, Role of amino acids in rheumatoid arthritis studied by metabolomics. International Journal of Rheumatic Diseases, (22) 2019. 38-46.
[94] A.E. Civitarese, S. Carling, L.K. Heilbronn, M.H. Hulver, B. Ukropcova, W.A. Deutsch, S.R. Smith, E. Ravussin, and C.P. Team, Calorie restriction increases muscle mitochondrial biogenesis in healthy humans. PLoS Med, (4) 2007. e76.
[95] A.M. Jenkinson, A.R. Collins, S.J. Duthie, K.W. Wahle, and G.G. Duthie, The effect of increased intakes of polyunsaturated fatty acids and vitamin E on DNA damage in human lymphocytes. Faseb j, (13) 1999. 2138-42.
[96] L. Mulderrig, J.I. Garaycoechea, Z.K. Tuong, C.L. Millington, F.A. Dingler, J.R. Ferdinand, L. Gaul, J.A. Tadross, M.J. Arends, S. O'Rahilly, G.P. Crossan, M.R. Clatworthy, and K.J. Patel, Aldehyde-driven transcriptional stress triggers an anorexic DNA damage response. Nature, (600) 2021. 158-163.
[97] M. Wang, F.A. Dingler, and K.J. Patel, Genotoxic aldehydes in the hematopoietic system. Blood, 2022. 139(14), 2119-2129.

Supplementary Information

Table S1. The information of lipid ISTDs.

Name	Concentration (mM)	Precursor Mass (M/Z)	Fragment Mass (M/Z)	Retention Time (min)
Analyzed by low pH LC-MS/MS method				
10-NO_2-OA-d_{17}	2.90	343.2	183.2	13.2
C18:1-ω9-d_{17}	3.34	298.1	298.1	13.8
C18:2-ω6-d_4	3.34	283.2	265.201	13.6
C22:6-ω3-d_5	1.50	332.1	288.4	13.4
C20:4-ω6-d_8	32.00	311.1	267.2	13.47
14,15-DiHETrE-d_{11}	0.29	348.2	207.1	9.8
5-i$PF_{2\alpha}$-VI-d_{11}	0.27	364.2	115.05	3.9
8,12-i$PF_{2\alpha}$-IV-d_{11}	0.27	364.21	115.05	5.9
12,13-DiHOME-d_4	0.31	317.2	185.1	9.3
8iso-PGE_2-d_4	0.28	355.3	275.25	5.42
8iso-$PGF_{2\alpha}$-d_4	0.28	357.3	197.15	4.75
9,10-DiHOME-d_4	0.31	317.2	203.1	9.5
9-HODE-d_4	0.33	299.2	172.1	11.1
LTB_4-d_4	0.29	339.5	197.1	9.2
PGE_2-d_4	0.28	355.3	275.25	4.8
$PGF_{2\alpha}$-d_4	0.28	357.3	197.15	4.75
TXB_2-d_4	0.27	373.5	173.3	3.7
20-HETE-d_6	0.31	325.2	279.2	10.6
12-HETE-d_8	0.30	327.2	184.1	11.7
5-HETE-d_8	0.30	327.1	116.15	12.1

Table S2. The information of energy production related metabolites ISTDs.

Name	Concentration	Molar mass (M/Z)	Retention Time (min)
ATP-$^{13}C_{10}$, $^{15}N_5$	10 mg/mL	520.9885	8.0
AMP-$^{13}C_{10}$, $^{15}N_5$	10 mg/mL	361.0558	4.2
Pyruvate-$^{13}C_3$	500 mM	90.0188	2.2
Succinate-d_4	500 mM	121.0444	3.7
UMP-$^{15}N_2$	500 mM	325.0227	4.4
Valine-$^{13}C_5$	0.5 mg/mL	123.0863	3.5

Table S3. The information of analyzed pro-inflammatory, oxidative stress related, and muscle growth stimulation metabolites in mouse muscle samples.

Name	Precursor Mass (M/Z)	Fragment Mass (M/Z)	Retention Time (min)	ISTD	ChEBI ID
Analyzed by LC-MS/MS method for lipid metabolites (in section 2.6.1)					
LA (C18:2-ω6)	279.2	261.2	13.6	C18:2-ω6-d_4	17351
GLA (C18:3-ω6)	277.0	233.0	13.3	C18:2-ω6-d_4	28661
DGLA (C20:3-ω6)	305.1	261.0	13.7	C20:4-ω6-d_8	NA
AA (C20:4-ω6)	303	259.0	13.5	C20:4-ω6-d_8	15843
AdA (C22:4-ω6)	331.5	287.5	13.8	C22:6-ω3-d_5	NA
PGD_2	351.1	271.15	5.1	PGE_2-d_4	15555
PGE_2	351.1	271.15	4.8	PGE_2-d_4	15551
$PGF_{2\alpha}$	353.1	193.1	4.6	$PGF_{2\alpha}$-d_4	15553
TXB_2	369.2	169.1	3.8	TXB_2-d_4	28728
9-HODE	295.2	171.1	11.1	9-HODE-d_4	72651
13-HODE	295.2	195.2	11	9-HODE-d_4	72639
12(S)-HETrE	279.2	179.1	9.8	12-HETE-d_8	90771
11-HETE	319.2	167.1	11.6	12-HETE-d_8	72606
15-HETE	319.2	219.2	11.3	5-HETE-d_8	64017
20-HETE	319.2	289.2	10.6	20-HETE-d_6	34306
5-HETE	319.2	115.15	12.3	5-HETE-d_8	28209
8-HETE	319.2	155.1	11.8	5-HETE-d_8	34486
9-HETE	319.2	167.1	12	12-HETE-d_8	72786
12-HETE	319.2	179.2	11.8	12-HETE-d_8	19138
Analyzed by HILIC-MS method (in section 2.6.2)					
GSH	306.0765 (M/Z)		4.5	Succinate-d_4	16856
GSSG	611.1447 (M/Z)		7.4	Succinate-d_4	17858

Table S4. The information of analyzed anti-inflammatory metabolites in mouse muscle samples.

Name	Precursor Mass (M/Z)	Fragment Mass (M/Z)	Retention Time (min)	ISTD	ChEBI ID
Analyzed by LC-MS/MS method for lipid metabolites (in section 2.6.1)					
ALA (C18:3-ω3)	277.1	233.15	3.9	C18:2-ω6-d_4	27432
EPA (C20:5-ω3)	301.1	257.2	13.3	C20:4-ω6-d_8	28364
DPA (C22:5-ω3)	329.2	285.4	4.7	C22:6-ω3-d_5	NA
DHA (C22:6-ω3)	327.1	283.1	13.4	C22:6-ω3-d_5	28125
12,13-DiHODE	311.2	293.15	8.46	9-HODE-d_4	88461
14,15-DiHETE	335.2	207.1	9.1	14,15-DiHETrE-d_{11}	88459
17,18-DiHETE	335.2	247.1	8.9	14,15-DiHETrE-d_{11}	88349
TXB_1	371.2	171.1	3.3	TXB_2-d_4	73994
PGF_1	355.2	311.1	4.75	$PGF_{2\alpha}$-d_4	28852
11,12-EET	319.22	167.1	12.8	14,15-DiHETrE-d_{11}	34130
14,15-EET	319.21	219.2	12.5	14,15-DiHETrE-d_{11}	34157
8,9-EET	319.21	155.1	12.8	14,15-DiHETrE-d_{11}	34490
12-HEPE	317.2	179.1	10.8	12-HETE-d8	88345
15-HEPE	317.2	219.2	10.6	5-HETE-d_8	72627
18-HEPE	317.2	299.2	10.4	12-HETE-d8	72802
5-HEPE	317.2	115.2	11.1	5-HETE-d_8	72801
9-HEPE	317.2	167.25	10.9	12-HETE-d_8	89570
PGE_1	353.2	317.2	5.15	PGE_2-d_4	15544
PGE_3	349.2	269.2	3.34	PGE_2-d_4	28031
Analyzed by HILIC-MS method (in section 2.6.2)					
β-hydroxybutyrate	103.0401 (M/Z)		2.3	Pyruvate-$^{13}C_3$	20067

Table S5. The information of analyzed energy production and storage related metabolites in mouse muscle samples.

Metabolites name	ChEBI ID	Detected Mass (M/Z)	Retention time (min)	ISTD
Analyzed by LC-MS/MS method for lipid metabolites (in section 2.6.1)				
Myristic acid (C14:0)	28875	227.2>209.2	11.6	C18:1-ω9-d_{17}
Palmitic acid (C16:0)	15756	255.2>237.2	13.8	C18:1-ω9-d_{17}
Stearic acid (C18:0)	28842	283.2>265.2	14.1	C18:1-ω9-d_{17}
Analyzed by HILIC-MS method (in section 2.6.2)				
Glucose	17234	179.0561	4.0	Succinate-d_4
Glucose-1-P	58601	259.0224	5.9	Succinate-d_4
Glucose-6-P	14314	259.0224	6.5	Succinate-d_4
Fructose-6-P	78697	259.0224	6.2	Succinate-d_4
Pyruvate	15361	87.0088	2.2	Pyruvate-$^{13}C_3$
Acetyl-CoA	15351	808.1185	0.9	Succinate-d_4
Citrate	16947	191.0919	8.1	Succinate-d_4
Cis-Aconitate	16383	173.0085	3.8	Pyruvate-$^{13}C_3$
α-Ketoglutarate	80619	145.0142	3.9	Succinate-d_4
Succinate	30779	117.0193	3.7	Succinate-d_4
Succinyl-CoA	15380	866.1312	4.8	Succinate-d_4
Malate	25115	133.0142	5.1	Succinate-d_4
Fumarate	37154	115.0037	4.4	Succinate-d_4
Alanine	15570	90.0550	4.6	Valine-$^{13}C_5$
Phosphocreatine	17287	210.0285	6.1	Succinate-d_4
Creatine	16919	130.0622	4.6	Succinate-d_4
ATP	15422	505.9885	8.0	ATP-$^{13}C_{10}$, $^{15}N_5$
ADP	16761	426.0221	7.2	AMP-$^{13}C_{10}$, $^{15}N_5$
AMP	16027	346.0558	4.2	AMP-$^{13}C_{10}$, $^{15}N_5$
6-phosphogluconate	48928	275.0174	7.1	Succinate-d_4
Riboluse-5-P	17363	229.0118	4.9	Succinate-d_4
Ribose-5-P	78679	229.0119	5.1	Succinate-d_4